LAWRENCE
LIVERMORE
NATIONAL
LABORATORY

UCRL-TR-207101

Analyses in Support of Z-IFE: LLNL Progress Report for FY-04

W.R. Meier, R.P. Abbott, J.F. Latkowski, R.W. Moir, S. Reyes, R.C. Schmitt

October 8, 2004

This work was performed under the auspices of the U.S. Department of Energy by University of California, Lawrence Livermore National Laboratory under Contract W-7405-Eng-48.

Analyses in Support of Z-IFE

LLNL Progress Report for FY-04

W.R. Meier, R.P. Abbott, J.F. Latkowski,
R.W. Moir, S. Reyes, R.C Schmitt

September 30, 2004

Contents

1. Introduction

During the last quarter of FY2004, Lawrence Livermore National Laboratory (LLNL) conducted a brief study of power plant options for a z-pinch-based inertial fusion energy (Z-IFE) power plant. Areas that were covered include chamber design, thick-liquid response, neutronics and activation, and systems studies. This report summarizes the progress made in each of these areas, provides recommendations for improvements to the basic design concept, and identifies future work that is needed.

As a starting point to the LLNL studies, we have taken information provided in several publications and presentations.[1-4] In particular, many of the basic parameters were taken from the ZP-3 study, which is described in reference 4. The ZP-3 design called for 12 separate target chambers, with any 10 of them operating at a given time. Each chamber would be pulsed at a repetition rate of 0.1 Hz with a target yield of 3 GJ. Thus, each chamber would have a fusion power of 300 MW for a power plant total of 3000 MW. The ZP-3 study considered several options for the recyclable transmission lines (RTL).

Early in the study, the LLNL group questioned the use of many chambers as well as the yield limitation of 3 GJ. The feeling was that a large number of chambers would invariably lead to a considerably higher system cost than for a system with fewer chambers. Naturally, this trend would be somewhat offset by the increased availability that might be possible with many chambers. Reference 4 points out that target yields as high as 20 GJ would be possible with currently available manufacturing technology. The LLNL team considered yields ranging from 3 to 20 GJ. Our findings indicate that higher yields, which lead one to fewer chambers, make the most sense from an economic point of view. Systems modeling, including relative economics, is covered in Section 2.

Regardless of the number of chambers of the fusion yield per target, a Z-IFE power plant would make use of a thick-liquid wall protection scheme. In this type of system a neutronically thick liquid is interspersed between the target and the first structural wall. By doing this, one is able to reduce the neutron damage to the wall to a point at which the wall becomes a lifetime component. This serves to reduce the power plant waste volume (and intensity) as well as increasing the plant availability. We find that a line density of ~1 m is needed to reduce the neutron displacement rate to acceptable levels.

When a thick-liquid protection scheme is used, several phenomena give rise to significant liquid motion. These include venting, ablation and isochoric heating. Each can lead to strong shocks. Liquid motion and chamber pressurization can cause large stresses, against which the chamber must act. The liquid and chamber responses are covered in Section 3.

Another area of innovation is in the selection of the chamber and RTL materials. The ZP-3 design calls for the use of a ferritic steel chamber and carbon steel RTLs. We assume an RTL mass of 50 kg. A significant drawback to a ferritic steel chamber is the inability to operate at high temperatures. Ferritic steel is typically limited to 600ºC, with some hope of extending to slightly higher temperatures in the future. This maximum temperature limits the overall thermal

efficiency to <40%. Another concern is the use of carbon steel RTLs, as debris would precipitate out on chamber surfaces. Instead, the LLNL team proposes the possible use of a carbon-carbon composite such as that originally proposed in the SOMBRERO reactor study.[5] A carbon composite would allow one to go to considerably higher temperatures, thereby increasing the thermal efficiency and/or making it possible to couple the Z-IFE power plant to a high-efficiency hydrogen production system. Thermal efficiencies of 51-64% might be possible with a helium secondary loop using a Brayton cycle.[6] Hydrogen cracking via the sulfur-iodine cycle could be done at ~50% for a secondary coolant temperature of 850ºC.[7]

In addition to attaining higher thermal efficiencies, a carbon composite chamber can be operated with a molten salt that is in an "oxidized" state (e.g., flibe that is beryllium poor). The salt would act as an oxidizing agent, thereby dissolving the RTL material and simplifying its handling and recycling. Additionally, the unburned and newly bred tritium would be oxidized to form tritium fluoride. Although corrosive, handling of tritium as TF is easier than in its T_2 form. TF has a much lower permeation in chamber materials, and thus, it should be easier to control the tritium inventory.

In Section 4, we cover the neutron transport and activation issues for Z-IFE. Options for the liquid layout are discussed, and the resulting spatially-dependent neutron doses are shown. We completed a neutron activation scoping study for alternative RTL materials and provide results for the waste disposal rating and contact dose rate for each chemical element. Finally, flibe activation is analyzed and possible alternatives to flibe are discussed.

Section 5 summarizes our proposed design modifications and details our recommendations and priorities for future work on Z-IFE.

During the course of this study, Mathcad workbooks were created to aid in the analysis of the systems modeling and the liquid and chamber response. Copies of these Mathcad workbooks are included as Appendices A and B. Finally, some miscellaneous calculation and considerations are documented in Appendix C.

References for Section 1

[1] C.L. Olson, "Progress on Z-pinch IFE and HIF Target Work on Z," 15th Int. Symp. on Heavy Ion Inertial Fusion (Princeton University Princeton, NJ June 7-11, 2004).

[2] C.L. Olson, "Z-pinch IFE Program," 2002 Snowmass Fusion Summer Study (Snowmass, CO July 8-19, 2002).

[3] C.L. Olson, "Inertial Confinement Fusion: Z-Pinch," Chapter 9 to be published.

[4] G. E. Rochau et al., "ZP3, A Power Plant Utilizing Z-Pinch Fusion Technology," Proceedings of the 2nd International Conference on Inertial Fusion Sciences and Applications (Sep. 2001), Kyoto, Japan.

[5] W. R. Meier et al., "Osiris and SOMBRERO Inertial Confinement Fusion Power Plant Designs," W. J. Schafer Associates, Inc., DOE/ER/54100-1, WJSA-92-01 (1992).

[6] R. Schleicher, A. R. Raffray, and C. P. Wong, "An Assessment of the Brayton Cycle for High Performance Power Plants," *Fusion Technol.* **39** (2001) 823-7.

[7] P. M. Mathias and L. C. Brown, “Thermodynamics of the Sulfur-Iodine Cycle for Thermochemical Hydrogen Production,” Presented at the 68th Annual Meeting of the Society of Chemical Engineers, Japan (March 2003).

2. Preliminary Systems Model for Z-IFE Power Plant

2.1 Introduction

A very crude systems model was created in order to investigate the design space for Z-IFE power plants. The base case Z power plant has 10 chambers and power units supplied by a central target/RTL manufacturing plant. (Actually, previous Sandia descriptions call for 12 units, with only 10 operating while two are maintained. This is likely an unnecessarily conservative assumption.) Each chamber produces 10% of the plant output power, typically assumed to be ~ 1 GWe. In our systems model we examine the cost of electricity (COE) as a function of the driver energy, chamber rep-rate and the number of units making up the power plant.

2.2 Description of the Model

The attached MathCad model (see Appendix A) includes all the model assumptions and comments in an easily readable format. The key points are summarized here.

Target Gain and Yield

Previous presentations and reports on Z-IFE gave some example target designs and predicted target yields.[1-3] We have fit a simple scaling equation to three cases for the dynamic hohlraum. The (x-ray energy, target yield) results for these targets were reported as (12 MJ, 0.53 GJ), (30 MJ, 3.0 GJ), and (37 MJ, 4.4 GJ). If we define the target gain as the yield divided by x-ray energy, the corresponding gains are 44, 100, and 119. These points are well fit by a simple scaling,

$$G = 100 \cdot (E_d/30)^{0.825}$$

where E_d is the driver produced x-ray energy in MJ. The exponent is chosen to fit the 30 MJ and 37 MJ cases and results in a small over estimate (6%) at 12 MJ. This exponent should be verified with more target modeling work. For direct-driver laser IFE, exponent is closer to 0.6 [Ref. 4]. The target yield is simply the product of driver energy and target gain,

$$Y = E \cdot G \ .$$

Power Balance Assumptions

The net electric power for the Z-IFE plant is given in the next section of the MathCad model. We have accounted for the additional power resulting from neutron reactions with chamber materials (+14%), subtracted the driver power input requirement, and have made allowance for other in-plant (auxiliary) electric power needs (-4% of gross power is typical). The driver efficiency (wall plug to x-rays) is assumed to be 15% and the thermal-to-electric conversion efficiency is taken as 50% corresponding to a high temperature chamber design. We have not made any estimate of the power requirements of the target/RTL manufacturing plant, which could be significant since it involves processing molten steel (at least for one approach for the RTLs). As an example reference case, we have the following parameters:

Driver x-ray energy, E_d = 25 MJ
Target gain, G = 86
Target yield, Y = 2.15 GJ
Chamber rep-rate, RR= 0.1 Hz
Number of units, N_u = 10
Fusion power, P_f = 2151 MWt (total for 10 unit plant)
Thermal power, P_t = 2452 MWt
Gross electric power, P_g = 1226 MWe
Auxiliary power, P_{aux} = 49 MWe
Driver power, P_d = 167 MWe
Net electric power, P_{net} = 1010 MWe

The driver energy was selected to give a net electric power of ~ 1GWe for a 10 unit plant when each chamber operated at 0.1 Hz. The yield in this example (2.15 GJ) is lower than the 3.0 GJ often cited in SNL documents due to different assumptions including accounting for neutron energy multiplication, using higher energy recovery fraction in the chambers (100% here), and using higher thermal conversion efficiency.

Cost Scaling Assumptions

In the absence of actual cost estimates (which were not available at the time we did this study), we made some rough assumptions on the relative costs of the major subsystems of the power plant: the drivers, chambers and power units, and target factory. These assumptions can easily be changed and eventually replaced with actual cost estimates for Z-IFE. The assumptions are as follows:

- Ten drivers account for 10% of the plant capital cost. This cost scales linearly with driver energy per unit and number of units, N_u:
  $C_d = 0.1 \cdot (E_d/25) \cdot (N_u/10)$, where E_d is the driver energy in MJ.

- Ten chambers account of 10% of the plant cost. This cost scales as the target yield raised to the 0.67 power and linear with the number of units:
  $C_{ch} = 0.1 \cdot (Y/2151)^{0.67} \cdot (N_u/10)$, where Y is the target yield in MJ.

- The power conversion system cost is 60% of the plant cost and scales as the total gross electric power raised to the 0.8:
  $C_{pp} = 0.6 \cdot [(P_{gu} \cdot N_u)/(123 \cdot 10)]^{0.8}$, where P_{gu} is each unit's gross electric power in MWe.

- The target factory cost is 20% of the plant cost and scales with the total production rate raised to the 0.7:
  $C_{tf} = 0.2 \cdot [(RR \cdot N_u)/(0.1 \cdot 10)]^{0.7}$, where RR is the chamber (unit) rep-rate in Hz.

2.3 Key Results

Capital Cost versus Driver Energy

The capital costs (for each subsystem and the total) as a function of driver energy are shown in Fig. 2.1 for a 10 unit, 1 GWe plant. The rep-rate is varied to maintain fixed net power as driver energy changes. The target factory cost dominates at low driver energy since the rep-rate needed

to maintain 1 GWe output decreases rapidly with decreasing driver energy (gain and yield). The COE of electricity is assumed to be proportional to the total capital cost (sum of above), implying that fuel and maintenance costs are small in comparison or roughly proportional to capital cost as well. Based on these assumptions, the minimum total capital cost (and thus COE) occurs at a driver x-ray energy of ~30 MJ, slightly higher than the reference case point used in the normalization.

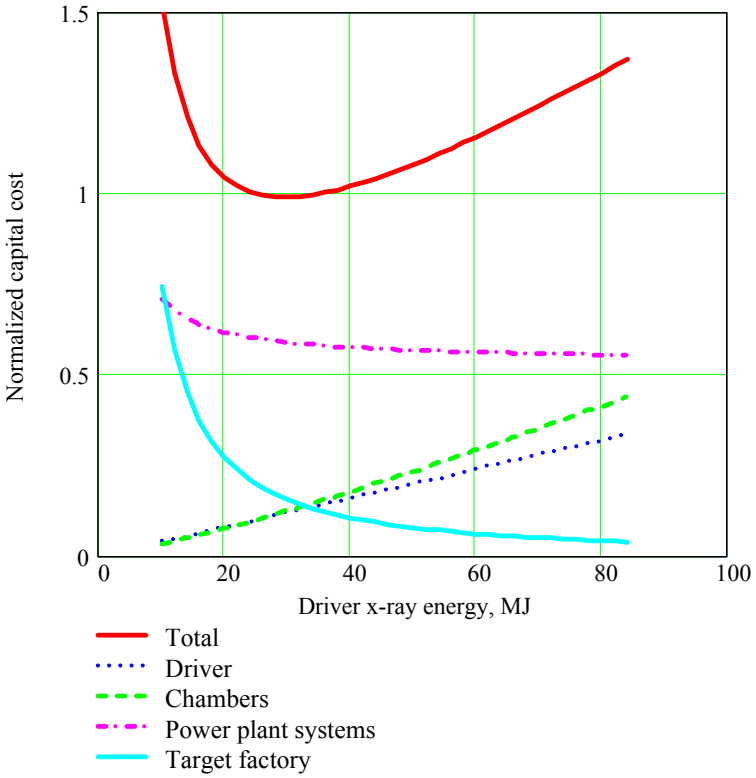

Fig. 2.1. Normalized capital cost versus driver x-ray energy for a 10 unit, 1 GWe plant. Contributions from major subsystems are shown.

COE versus Driver Energy for One, Five and Ten Unit Plants – Fixed Power

Figure 2.2 shows the normalized COE versus driver energy for 10, 5 and single unit plants. The rep-rate per chamber varies with driver energy to keep the plant net power fixed at 1.0 GWe. The circles on the curves indicate the 0.1 Hz per chamber design points (higher energy corresponds to lower rep-rate and vice versa). For fixed 0.1 Hz, the required driver x-ray energy for 10, 5 and 1 unit plants is 25 MJ, ~36 MJ and ~84 MJ, respectively, and the corresponding target yields are 2.15, 4.13, and 19.5 GJ. The normalized COE for these 0.1 Hz cases decreases with decreasing number of units from 1.00 at ten units, to 0.85 with five units to 0.67 with a single unit.

The minima occur at slightly different driver energies and rep-rates. The minima are at 30, 40 and 80 MJ for the 10, 5 and 1 unit plants, with rather broad ranges giving near optimal COEs.

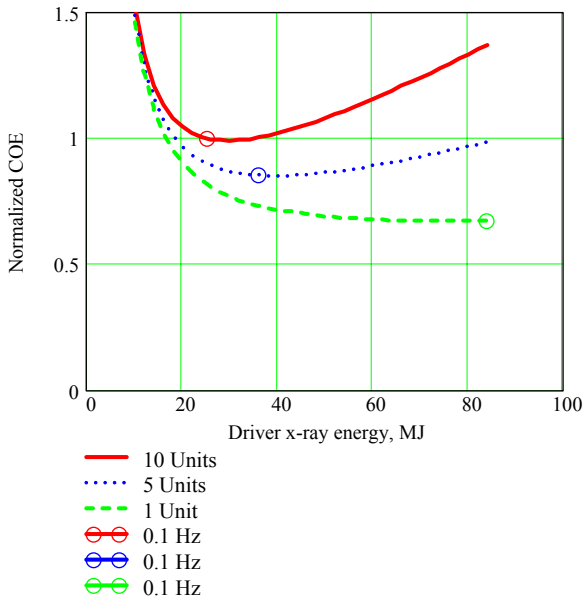

Fig. 2.2. Normalized COE versus driver x-ray energy for 1 GWe plants comprised of 10, 5 or 1 units. The circles indicate the driver energy corresponding to 0.1 Hz per chamber.

COE versus Rep-rate for One, Five and Ten Unit Plants – Fixed Power

The final comparison, shown in Fig. 2.3, is the COE as a function of rep-rate, again holding the net power of the plant fixed. The rep-rate for the minimum COE points are 0.070 Hz, 0.081 Hz, and 0.11 Hz for the 10, 5 and 1 unit plants, respectively.

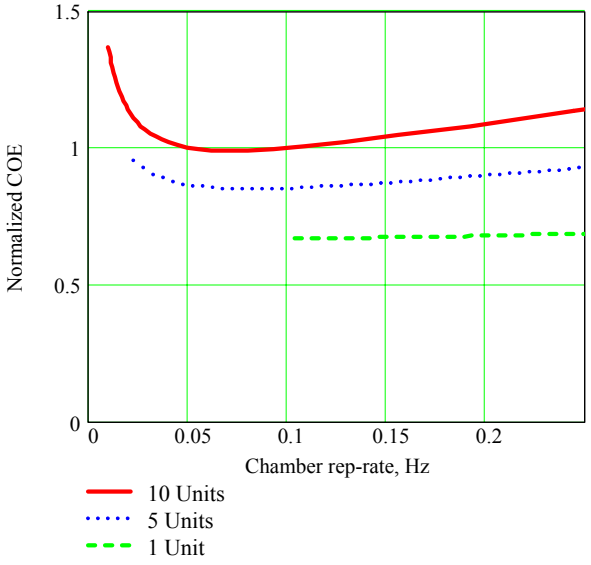

Fig. 2.3. Normalized COE versus chamber pulse repetition rate for 1 GWe plants comprised of 10, 5 or 1 units.

Summary of Optimum Points

The optimal designs for the 1 GWe plant are summarized in Table 2.1.

Table 2.1. Summary of Optimum Design Points for 1 GWe Plants

	10 units	**5 Units**	**1 Unit**
Driver x-ray energy, MJ	30	40	80
Target yield, GJ	3.0	5.1	18.0
Rep-rate per unit, Hz	0.070	0.081	0.109
Interpulse time, s	14.3	12.4	9.2
Normalized COE*	0.99	0.85	0.67

*Normalized to E_d = 25 MJ, Y = 2.15 GJ, RR = 0.1 Hz.

2.4 Conclusions

Based on this preliminary systems analysis of the z-IFE power plant, we conclude that there is potentially significant economic benefit of developing a plant that uses fewer than the nominal 10 units and higher yields (> 10 GJ) if feasible. The degree to which this is possible will depend on may other technical issues including the ability to deliver the high currents need for such high yields and the ability to design chambers to contain the blast. The results also show that somewhat lower chamber rep-rates (< 0.1 Hz) can be used with little impact on the COE. We caution, that these conclusion are based on very crude models that need to be improved in the next phase.

References for Section 2

[1] C.L. Olson, "Z-pinch IFE Program," 2002 Snowmass Fusion Summer Study (Snowmass, CO July 8-19, 2002).

[2] C.L. Olson, "Inertial Confinement Fusion: Z-Pinch," Chapter 9 to be published.

[3] C.L. Olson, "Progress on Z-pinch IFE and HIF Target Work on Z," 15th Int. Symp. on Heavy Ion Inertial Fusion (Princeton University Princeton, NJ June 7-11, 2004).

[4] L.J. Perkins, "Target Design Activities for the High Average Power Laser Program – Gain Curves," HAPL Project Meeting, Sept. 24-25, 2003, University of Wisconsin, Madison WI. http://aries.ucsd.edu/HAPL/MEETINGS/0309-HAPL/program.html

3.0 Shock Mitigation by Liquid Jets and Peak First Wall Stress

3.1 Introduction

There are several phenomena in liquid protected IFE target chambers that lead to forces being imposed upon the shielding jet arrays. In some chases, the motion caused by these forces results in liquid slapping against the first structural wall (FSW) and causing potentially damaging mechanical stresses. This document serves as an introduction to an associated Mathcad document (Appendix B) quantifying the magnitude of this threat for shielding geometry particular to a Z-IFE target chamber. Appendix B gives more detail than the summary here, including the complete set of equations and assumptions. Results from several computations with this Mathcad document are included as examples.

The liquid shielding geometry called for in Z-IFE is quite similar to the concepts employed in both the HYLIFE and HYLIFE-II reactor studies.[1,2] Consequently, much of the analysis previously carried out to understand the dynamics of these chambers can be applied to the current situation.

The HYLIFE chamber used 1.8 GJ targets yields and employed an annular array of lithium jets to provide neutron and shock attenuation for the FSW. A series of papers published by Glenn and shock tube experiments conducted by Liu, Peterson, and Schrock[3,4] document and verify the effectiveness of this geometry in mitigating shocks, with further confirmation provided by the 2-D hydro-code TSUNAMI.

In HYLIFE-II, the lithium shielding was replaced by flibe and target yields were reduced to 350 MJ. Even though the processes that result in liquid motion were still present, the induced outward liquid motion was reduced to a level that it did not hit the FSW avoiding impact stress. Unfortunately, this will not be the case for a reasonably sized Z-IFE target chamber and its much larger target yields.

Liquid Ablation

About 30% of the energy released from a Z-IFE target will be in the form of x-rays and ionized debris. This energy will deposit in and ablate a thin layer of liquid from all target facing shielding surfaces [5]. This event will send a strong shock into the liquid as the ablated plasma rockets toward the center of the chamber. This shock will contribute to liquid motion toward the FSW and the stresses that will result.

The specific ablation impulse can be shown to be

$$I = \frac{\sqrt{2 \cdot m_p \cdot E}}{A}$$

where (m_p) is the ablated mass, (E) is its kinetic energy, and A is the surface area of the shielding pocket surrounding the fusion target. When divided by the aerial density of the shielding (μ) (amount of mass for each unit of pocket surface area) we get the induced velocity from liquid ablation

$$v_a = \frac{I}{\mu}$$

For a 12-m-diameter Z-IFE chamber employing targets with 3 GJ yields and protected by an annular array of jets like that shown in Fig. 3.1, the resulting liquid velocity toward the FSW will be approximately 0.25 m/s. If the same chamber and shielding is used along with larger 20 GJ targets, the outward liquid velocity will grow to 1.30 m/s. Note that the chamber and jet array dimensions were chosen early in our studies to investigate neutronics effects (see Section 4). As will be seen later, in terms of withstanding liquid impact induced stress, the configuration is too robust for 3 GJ yield targets, but will require modifications (e.g. larger radius, thicker wall, etc.) to withstand 20 GJ yield. The will be the subject of further work in FY05.

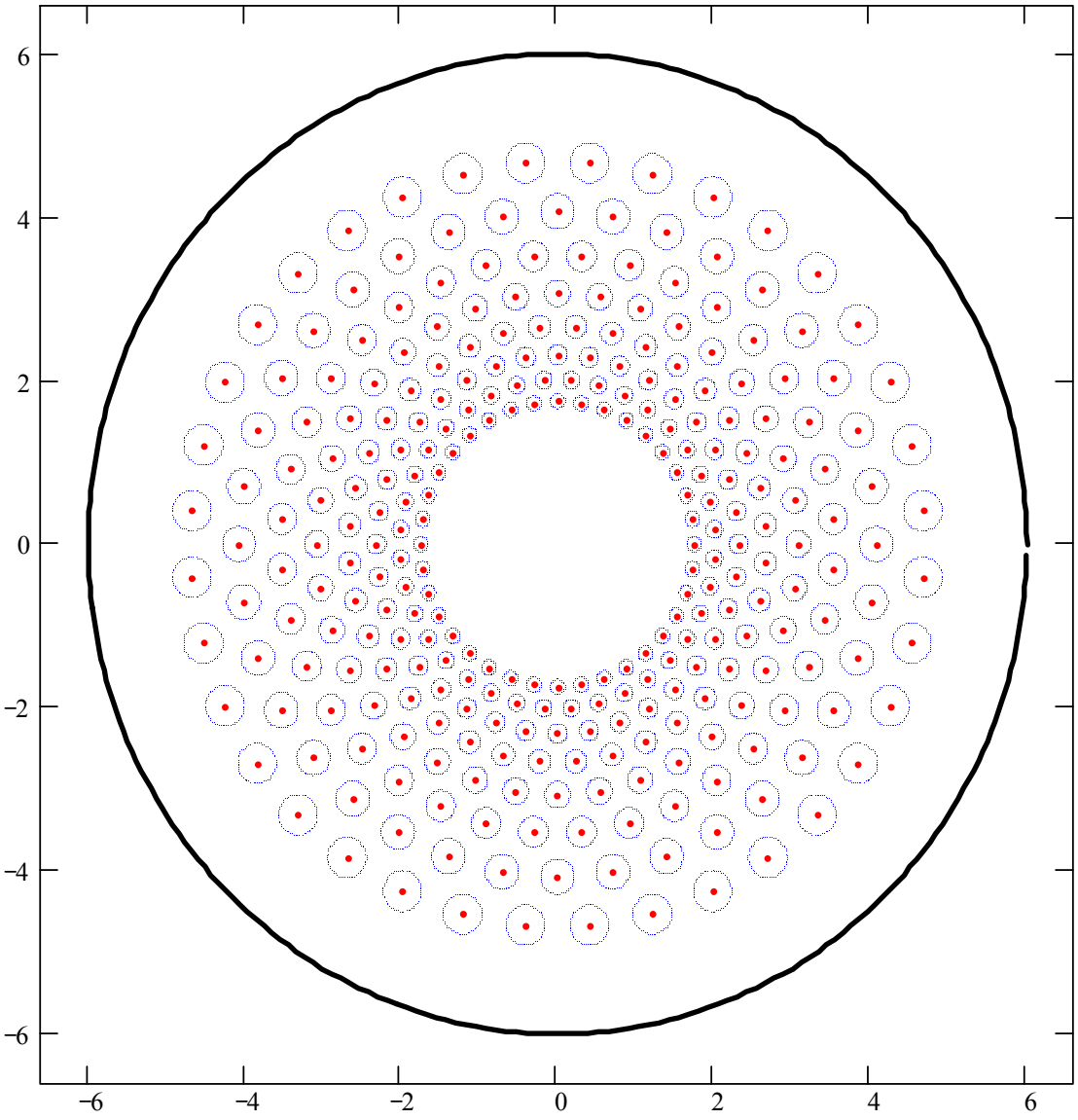

Fig. 3.1. An annular array of flibe jets with inner pocket radius of 1.5 m, 66 % void fraction, and 3 m thickness protecting a 12 m diameter cylindrical Z-IFE target chamber.

Pocket Pressurization and Venting

After the initial liquid ablation has occurred, the plasma generated will cool by re-radiating to newly exposed target facing liquid surfaces and produce further vaporization. This gas will then vent through the liquid shielding array over some period of time and impose a form drag. This drag will further accelerate the shielding liquid toward the wall. The amount of additional induced velocity from venting will be

$$v_v = \frac{P_o \cdot \tau}{\mu}$$

where (P_o) is the initial pocket pressure and (τ) the venting time constant.

For the geometry shown above in Fig. 1, the induced liquid velocity will be 1.04 m/s using a 3 GJ target and 7 m/s using a 20 GJ target.

Neutron Isochoric Heating

Glenn has studied the mechanisms by which volumetric deposition of neutrons will impart bulk outward motion to liquid shielding and quantitatively determined the magnitude of that motion [3]. Further, he has shown that this effect will be reduced by 2/3 for an annular array shielding geometry due to dissipation by viscous forces. The induced velocity from neutrons based on Glenn's work [6] is then

$$v_n = \frac{0.3E \cdot \Gamma}{C \cdot m}$$

where (E) is the total deposited neutron energy, (Γ) is the Gruneisen constant, (C) the liquid sound speed, and (m) the total amount of mass in the annular shielding array.

For the geometry illustrated before in Fig. 1 and 3 GJ target yields the liquid velocity from this energy source is 1.05 m/s. For the 20 GJ target yield scenario, the liquid velocity increases to 7 m/s.

The final bulk liquid velocity toward the FSW will simply be the sum of the velocities induced by the mechanisms described above and derived in detail in the associated Mathcad document.

$$v = v_a + v_v + v_n$$

The stresses that result in the FSW will have a magnitude proportional to the magnitude of this induced velocity, which is 2.3 m/s at 3 GJ and 15.3 m/s at 20 GJ yield.

Peak Stresses in the FSW

The peak stresses in the FSW due to the bulk liquid motion can be determined from the expression

$$\sigma = \frac{v \cdot m}{t \cdot A} \cdot \sqrt{\frac{G}{2 \cdot \rho \cdot \left(1 - \nu^2\right)}}$$

given in Ref. 5, where (v) is the liquid velocity, (m) the total liquid mass, (t) is the wall thickness, (A) is the total wall area, (G) is the wall material's elastic modulus, (ρ) is its density, and (ν) is its associated poisson ratio. Table 3.1 summarizes these parameters for two proposed wall materials along with their yield (for FS) or tensile (for C-C) strengths.

Table 3.1. Material property table for two candidate Z-IFE FSW materials.

	Ferritic Steel	C-C Composite
Elastic modulus [GPa]	190	200
Density, [g/m^2]	7800	2000
Poission ratio, ν	0.3	0.3
Yield stress @ 600 °C [MPa]	300 [7]	
Tensile strength [MPa]		310 – 517 [8]

Table 3.2 shows resulting peak stresses in a 5 cm thick FSW for a Z-IFE target chamber with dimensions and shielding as described in Fig. 3.1 for both materials.

Table 3.2. Resulting peak FSW stresses for dimensions and shielding illustrated in Fig 3.1.

Yield	*FS*	*C-C*
3 GJ	*112 MPa*	*228 MPa*
20 GJ	*728 MPa*	*1.5 GPa*

The peak stress for the 3 GJ FS and 3 GJ C-C cases are below yield and tensile strengths of both of those materials, respectively, but the 20 GJ case (for this geometry at least) clearly presents a problem. Fatigue, even for the 3GJ case could still be an issue. There are several parameters that can be changed to reduce peak FSW stresses. The plots in Fig. 3.2 illustrate the effect of varying some key parameters from half to twice their nominal value on both induced liquid speed and peak FSW stress. The normalization values are yield = 3 GJ, pocket inner radius = 1.5 m, pocket height = 4 m, FSW thickness = 0.05 m. As expected, the impact induced stress is proportional to the target yield (Y). Increasing the chamber radius (Rc) and/or FSW thickness (t) have the greatest impact on reducing stress for a given yield. Increasing the liquid pocket inner radius (R) slightly reduces stress, while increasing the pocket height (H) increases stress due to higher liquid mass (see Mathcad code for details).

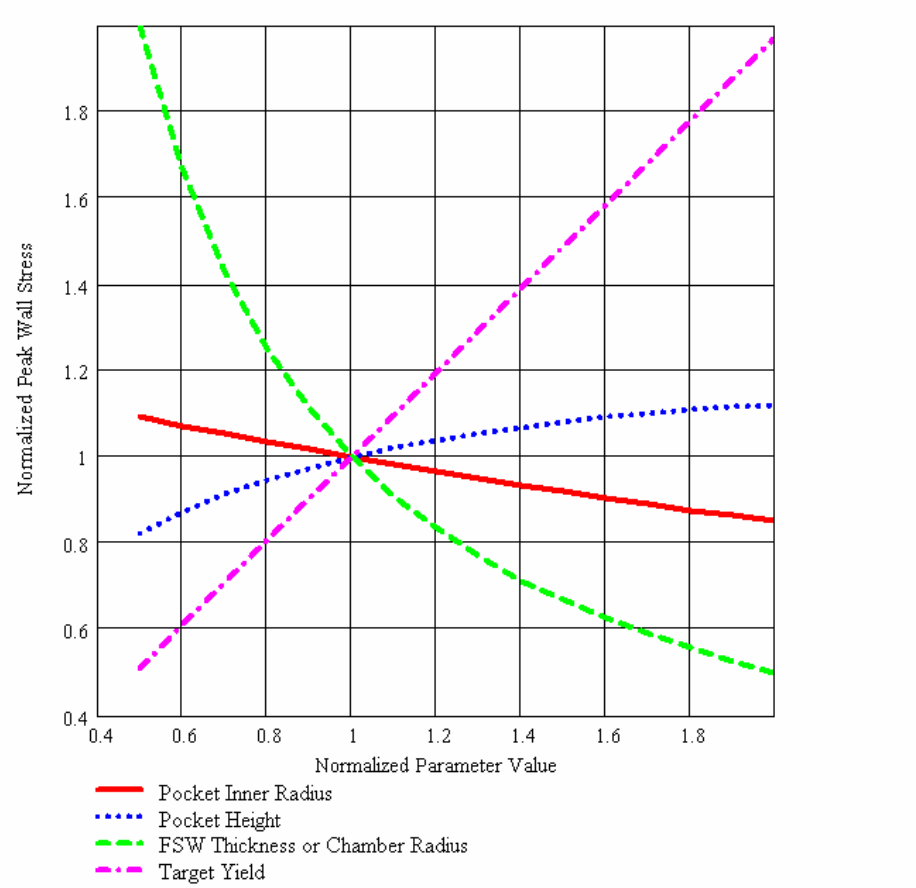

Fig. 3.2 Normalized effects of parameter variation on induced liquid speed and peak FSW stress. (Normalized to R = 1.5 m, H = 4, t = 0.05 m, Rc = 6 m, Y = 3 GJ)

References

[1] A. Blink, W. J. Hogan, J. Hovingh, W. R. Meier, and J. H. Pitts, "The high-yield lithium-injection fusion-energy (HYLIFE) reactor," UCRL-53559 (1985).

[2] R. W. Moir, R. L. Bieri, X. M. Chen, T. J. Dolan, M. A. Hoffman, P. A. House, R. L. Leber, J. D. Lee, Y. T. Lee, J. C. Liu, G. R. Longhurst, W. R. Meier, P. F. Peterson, R. W. Petzoldt, V. E. Schrock, M. T. Tobin, W. H. Williams, "HYLIFE-II: A Molten Salt Inertial Fusion Energy Power Plant Design-Final Report," *Fusion Technology* **25** (1994) 5-25.

[3] L. Glenn, references 17, 18, 19, 23 and 26 of Ref. 1.

[4] J. C. Liu, P. F. Peterson, and V. E. Schrock, "Blast venting through blanket material in the HYLIFE ICF reactor," Fusion Technology **21** (1992) 1514.

[5] R. W. Moir et al, "HYLIFE-II progress report," UCID-211816 (1991).

[6] R. Moir, "Chamber, target and final focus integrated design," Nucl. Instr. and Methods in Physic Res. **A 464** , 2001, 140-151.

[7] http://www-ferp.ucsd.edu/LIB/PROPS/FS/FS.html#2

[8] Buckley, Edie, eds. *Carbon-Carbon Materials and Composites***,** William Andrew Publishing/Noyes, 1993, p. 152.

4. Neutronics Analyses

4.1 Introduction

Designing a chamber for z-pinch driven inertial fusion power plant is a challenging problem and there are many issues that must be addressed. The large output from the fusion targets (~1-20 GJ yield/shot) leads to a large output of neutrons and blast shock. The chamber vessel containing these shots must be able to withstand significant blast shock and radiation damage for the life of the power plant (assumed to be 30 years). In order to bring the radiation doses down to acceptable levels for current materials (e.g., steels), a thick-liquid protection, usually composed of the molten-salt flibe, has been designed to protect the wall from significant neutron doses. Neutronics calculations, using the monte-carlo TART2002 [1] code from Lawrence Livermore National Laboratory (LLNL) were performed to model the neutron interactions with the system.

In using a z-pinch inertial fusion system, large amounts of power must be brought to the target. This power is delivered via recyclable transmission lines (RTLs) to the target. These RTLs must be able to handle on the order of 50-100 MA. The current RTL design calls for approximately 50 kg of iron to be molded into two concentric cones of approximate thickness of 100 microns. This study looks at the RTL material choice from a safety and environmental point of view. All elements on the periodic table were assessed according to waste disposal rating (WDR) and contact dose rate (CDR). The WDR allows us to determine the availability to shallow land burial after use, and the CDR allows us to calculate the dose to remote recycling equipment as the material is reformed into a new RTL for later shots. A small analysis was also done to look at whether these materials could be cleared and not require disposal.

The molten salt will see a large fluence of fusion neutrons, among other radiation from the target. These neutrons will cause the fluid to activate, causing the material to heat up. We have used the TART2002 code coupled with the ACAB fusion activation code to predict the decay heat for different choices of liquid protection material. The material was allowed to cool, and results are presented to show the thermal power given off by the activated material as a function of time after the fusion shot.

The issue of target material will prove to be an important issue when economics of the power plant are brought about. With significant amounts of high-Z material in the hohlraum and target, large masses of material are needed if new material is to be used for each target. Recycling the target material would be a big advantage, and may be necessary, for this type of power plant scheme.

4.2 Description of System

The z-pinch IFE idea is based upon delivering high pulsed power to a fusion target which then ignites and produces fusion yield. The heat and shock are dissipated through a thick blanket of liquid jets (e.g., ~3 m at 33% liquid fraction for 1 m equivalent thickness)and contained by a containment vessel wall. The thickness of the pocket of flibe is determined by calculating the effective dose to the first wall with different thicknesses of flibe. With 1 meter of flibe, the

carbon-carbon composite wall will survive adequately. The power from the system is generated by a conventional heat cycle by removing the heat from the exposed liquid.

Different schemes have been proposed for the correct number of chambers and fusion yield for each chamber. Due to economic considerations, we feel that having a single chamber with the largest acceptable yield is advantageous (see preliminary systems analysis in Section 2 of this report). Our proposed chamber geometry is a carbon-carbon composite cylindrical chamber with a 6 m radius and a height of 8 m. This chamber is designed to take 20 GJ yields and operate at 0.1 Hz, for a fusion power of 2000 MW. As shown in Fig. 4.1, there is a flibe jet array used to protect the chamber wall from damage. Many cylindrical jets have been used to mitigate the shock blast produced by the fusion explosion.

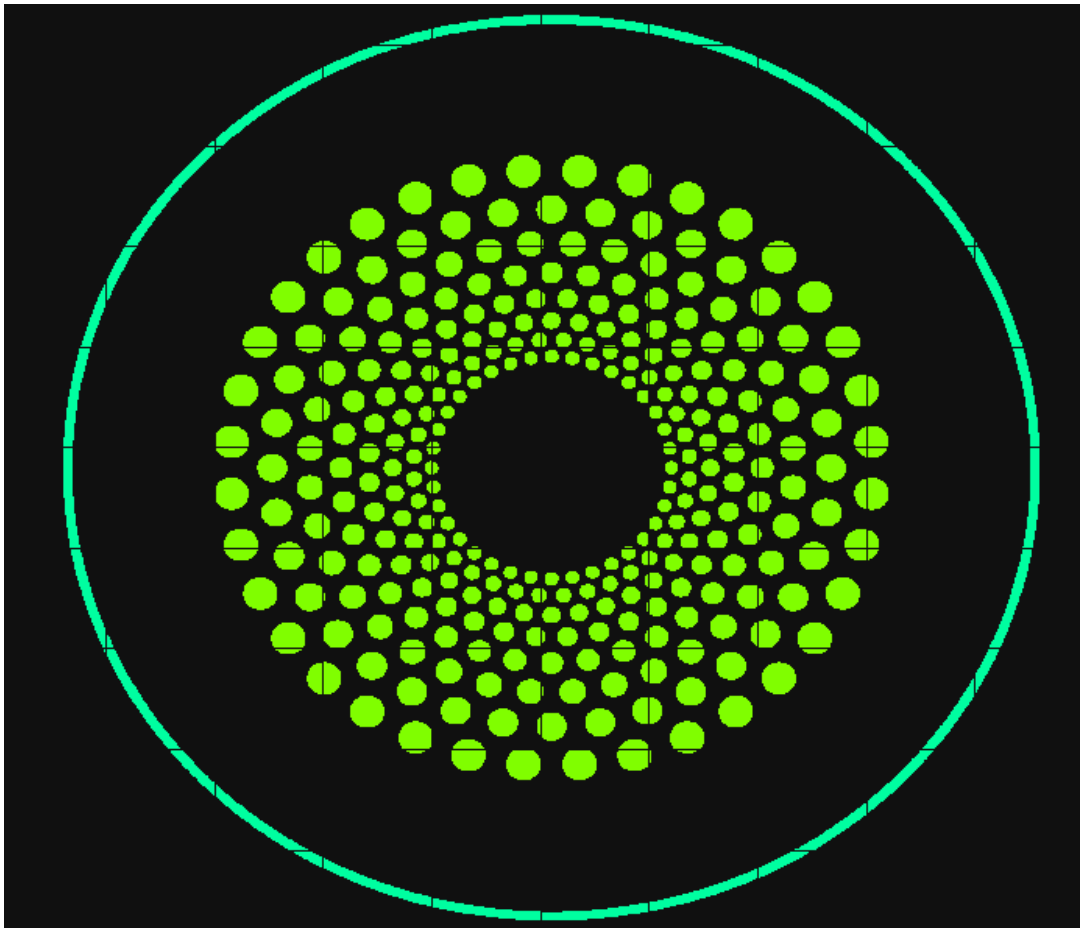

Figure 4.1. Flibe jet geometry. Horizontal cut at target plane.

Figure 2.2 is a ProEngineer sketch of a cutaway of our proposed chamber. Note that there is a 2 m deep flibe pool at the bottom of the chamber. This pool is used to collect all of the flibe dropping from the top of the chamber and to protect the bottom of the chamber from direct target output directed downward.

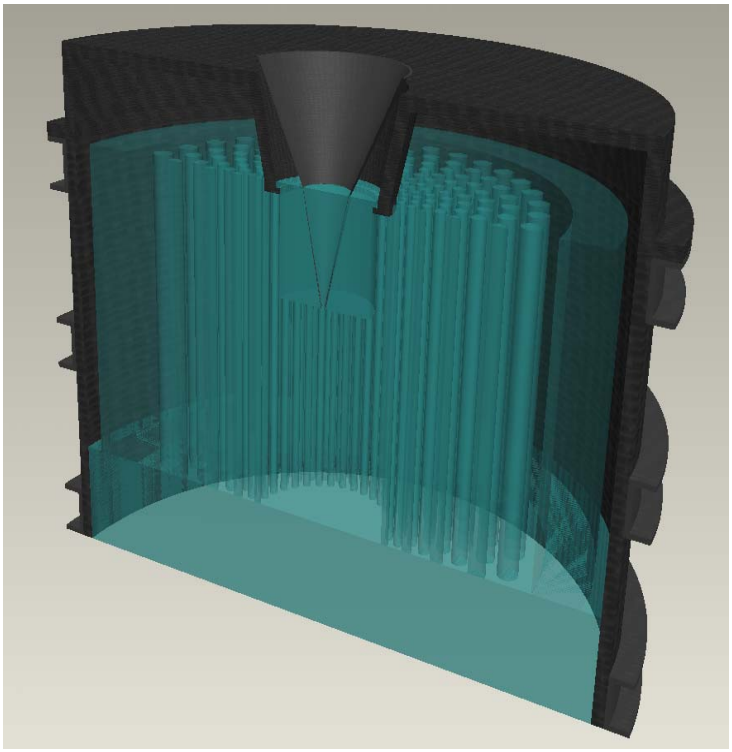

Fig. 4.2. Side Cut-away view of the z-pinch IFE chamber with flibe jet geometry.

4.3. Recyclable Transmission Line (RTL) Analysis

The recyclable transmission lines (RTLs) for the z-pinch IFE power plant idea allow large amounts of power to be transmitted to the target during a shot. The RTL must be capable of transmitting 10-100 MA through two concentric conical sheets of conducting material. The RTL must also be structurally capable of being brought in for each shot by some type of crane or holding device. With vacuum in the chamber of ~10-20 torr, stresses will be put on the RTL and the thickness and rigidity of the RTL must be able to withstand the forces present to it without distorting beyond an acceptable limit.

The current baseline case for RTL material is to use iron as the conducting material. Due to the required thickness (~100 microns) and size, these RTL's are approximately 50 kg [6]. Running the power plant at ~ 0.1 Hz per chamber times the number of chambers per plant creates a tremendous amount of material that is activated during the power plant lifetime. For this reason, we feel recycling of the RTL material will be necessary. Also, material choice for the RTL is very important from a safety and environmental perspective. Ideally, we want a material to be classified for shallow land burial (Class C waste). We also want the dose to remote handling equipment from activated RTL material to be low enough that the equipment lifetime is as long as the plant life.

Because of these requirements, a study of alternative RTL materials was performed. Each element on the periodic table was analyzed for waste disposal rating and contact dose rate to

remote handling equipment. Note that constant volume was used for each element, as the shape of the RTL will be similar no matter what choice of material is made. The neutron spectrum for the RTL was generated using the TART2002 code (a 3-D neutron-photon monte-carlo code). Using that neutron spectrum, each material was run through the ACAB activation code [2] using an automated process. Waste disposal rating data and contact dose rate information were extracted, and the results are plotted in Figures 4.3 and 4.4 below. For each element, the top half of the box assumes a weekly recycling scenario for the material. This would allow the material to cool in a holding area for 7 days before instantly being recycled and re-shot in the power plant. The lower section of each box assumes daily recycling, which may be required if t having 7 days of cooling creates too much waste inventory. These two scenarios will most likely bound actual recycling scenarios. Waste disposal ratings of less than or equal to 1 are acceptable for shallow land burial. A contact dose rate less than or equal to 114 Gy/h gives an acceptable lifetime dose to the machinery $<3 \cdot 10^7$ Gy [3]. As we can see many of the low atomic number elements are acceptable for our scenarios, but the higher atomic number elements would require significant engineering to be used.

Iron could be chosen as the RTL material from a safety and environmental point-of-view; however caution should be used with daily recycling, as the contact dose rate could be high enough to cause damage to operating equipment during the lifetime of operation. Materials such as a frozen flibe (BeF + LiF) could also be considered, as their activation characteristics are well below the limits of acceptability. Caution must be taken when looking at this data alone, as electrical conductivity is a key consideration when designing a RTL, as the power must be delivered to the target in a timely and efficient manner. We are merely presenting a view as one criterion to select the RTL material from.

4.4 Chamber Coolant Issues

Total inventory of flibe in one chamber is roughly 300 m^3. We assume that we will need on the order of 10 times that amount of flibe for a working system (may be even higher, as in the HYLIFE-II heavy-ion driven inertial fusion power plant concept [5]). Therefore all of our fluid models are based upon having a total inventory of flibe of approximately 3000 m^3. We calculated the decay heat in the flibe after 30 years of operation accounting for the average residence time in the neutron flux. As seen in Figure 4.5 the total power is very modest, less than 1 MW (compared to plant power of several thousand).

A study was completed to determine the amount of alternative liquids that would be required to equal the neutron shielding that 1 m of flibe protection offers. This thickness of flibe was chosen as to give a very low number of displacements (~10 dpa for 2000 MW fusion chamber) over the lifetime of the carbon-carbon composite first wall. This discussion will be saved for the next section. Both liquid lithium and liquid lithium-lead were looked at as alternatives. It was found through monte-carlo modeling that roughly 2.3 meters of liquid lithium would provide the same neutron shielding as the 1 meter of flibe. Also, nearly 6 m of liquid lithium-lead would be needed to provide adequate shielding of the chamber wall. This is clearly an unacceptable material, as the inventories of the liquid would be large and the power required to pump the liquid lead unacceptable. For now, it is recommended that flibe be considered as the active research material for chamber protection and heat removal.

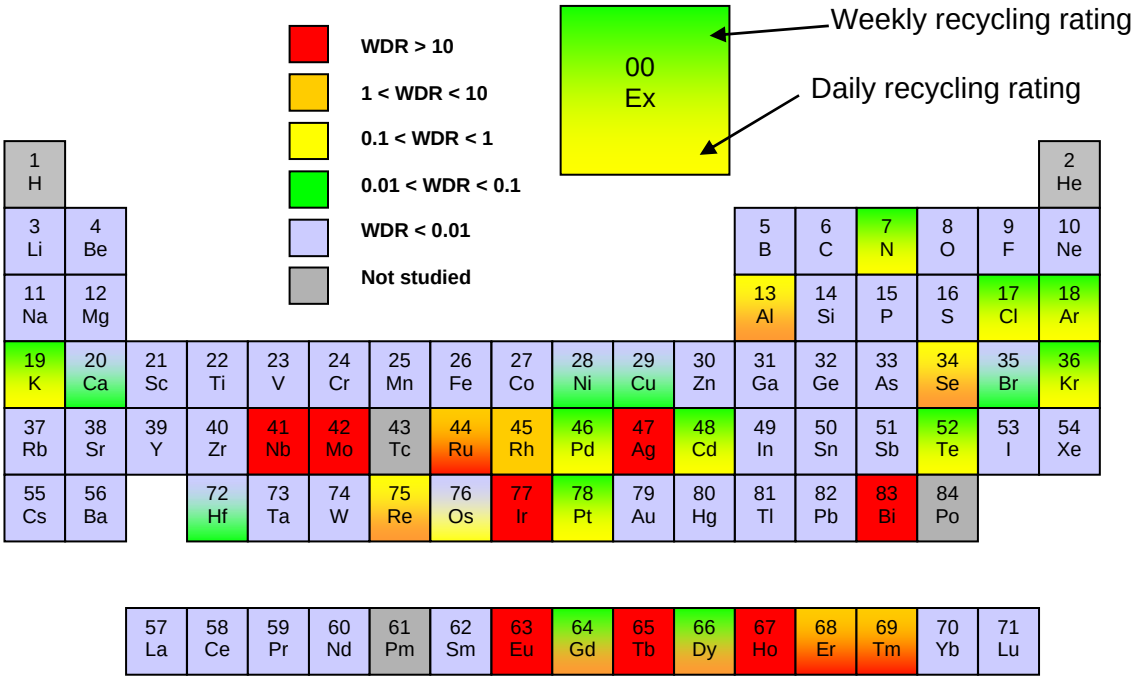

Fig. 4.3. Table of isotopes showing waste disposal rating for each element.

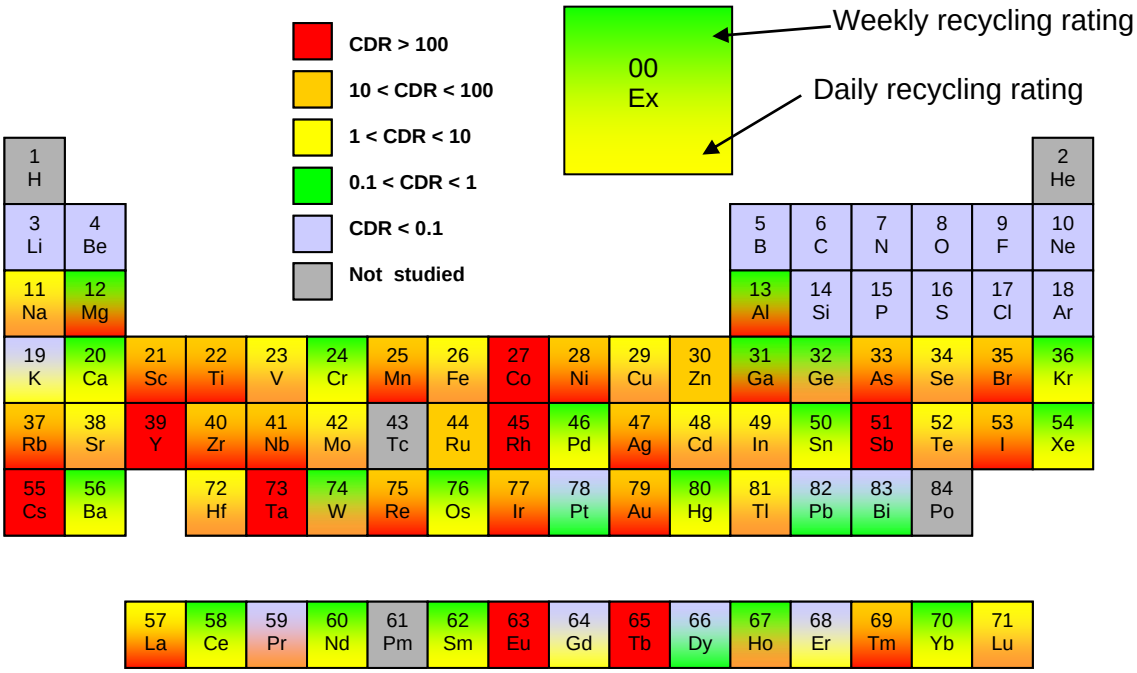

Fig. 4.4. Table of isotopes showing contact dose rate for each element

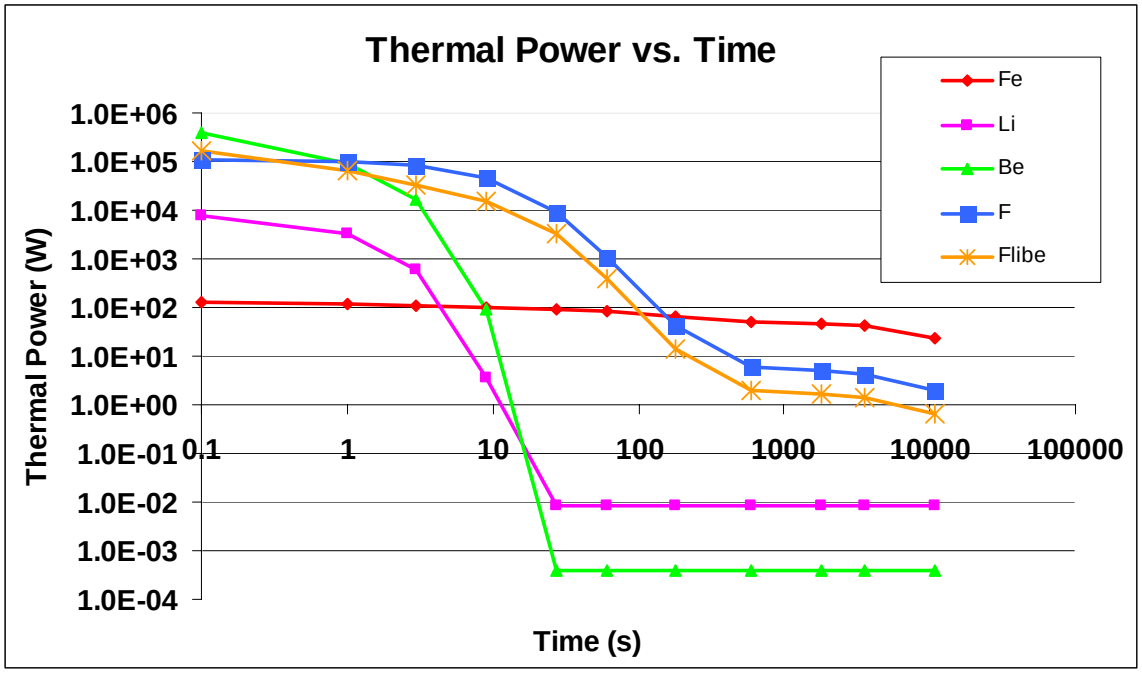

Figure 4.5. Graph of thermal power versus decay time for some power plant materials.

4.5 Containment Wall Issues

Different materials can be considered for the Containment wall for the z-pinch IFE power plant. As an advanced design case, we propose using a carbon composite wall that could be operated at higher temperatures than steel. An advanced Brayton cycle could then be used to get high thermal cycle efficiencies. The SOMBRERO study [4] looked at a carbon composite first wall for laser-driven inertial fusion energy. The wall in Sombrero was not protected by liquid jets so the neutron damage rate was high, on the order of 15 dpa per year of full power operation. After a few years (or less) swelling would require replacement of the first wall. Obviously, this is not attractive for a power plant situation, where plant availability is very important for the economics of the plant, and removing and replacing the chamber wall every few years could have a significant economic impact.

For this z-pinch IFE power plant using approximately 1 meter of flibe for shielding, we find an approximate carbon damage of less than 10 dpa for the 30-year full-power lifetime of the plant. As shown in Fig. 4.6 below, C/C initially experiences densification under neutron radiation followed by rapid swelling. At 10 dpa, the material has compacted by 0.05%, which seems to be acceptable for our situation.

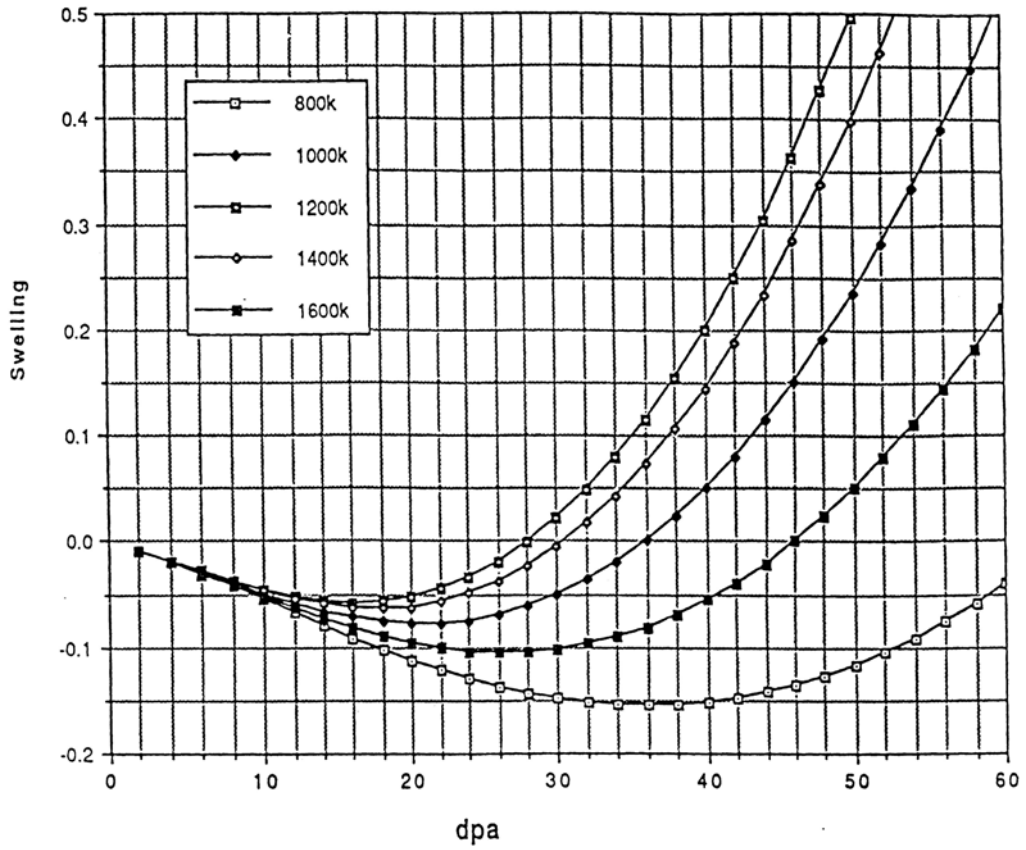

Fig. 4.6. Graphical representation of carbon swelling due to displacements from neutrons at various carbon temperatures.

Figure 4.7 is a plot of the dose as a function of height from the bottom to top of the chamber wall. It is averaged over all azimuthal angles. At low heights the dose is very small, due to the flibe pool sitting at the bottom of the chamber attenuating all of the radiation. The dose peaks near the target elevation of 612 cm. Figure 4.8 is a plot of the dose azimuthally around the chamber. This shows the dose for the 360 degrees around the target at the height of the largest dose from the previous plot. The dose is quite uniform, varying by less than 10% around the chamber.

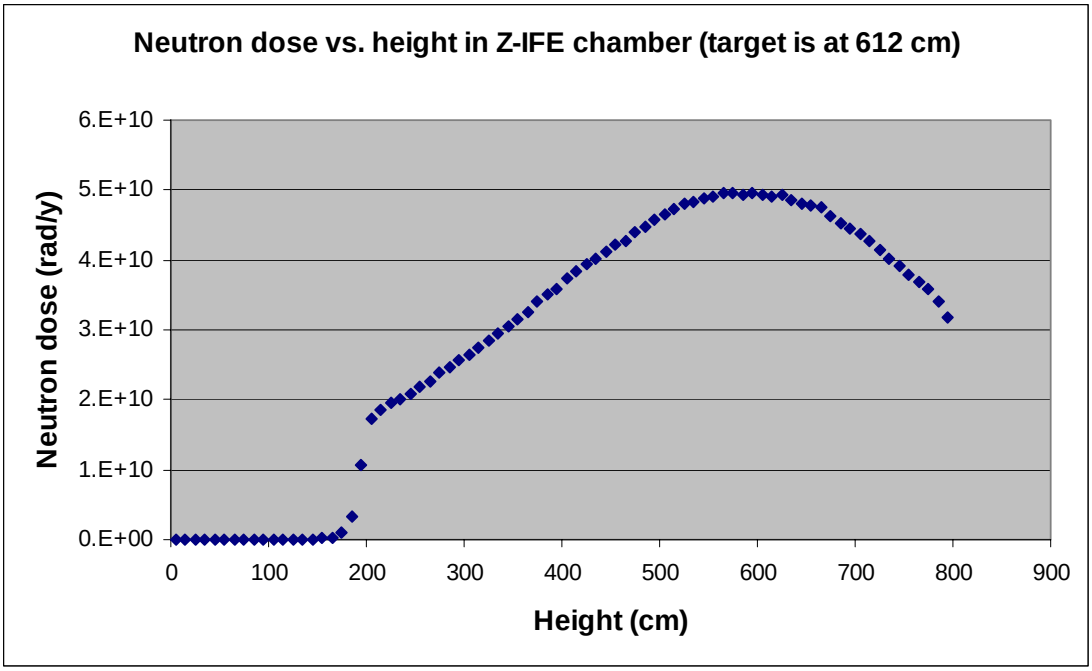

Fig. 4.7. Graph of neutron dose (rad/y) versus the vertical position on the chamber wall. Notice that the peak dose occurs at an elevation slightly below the target plane.

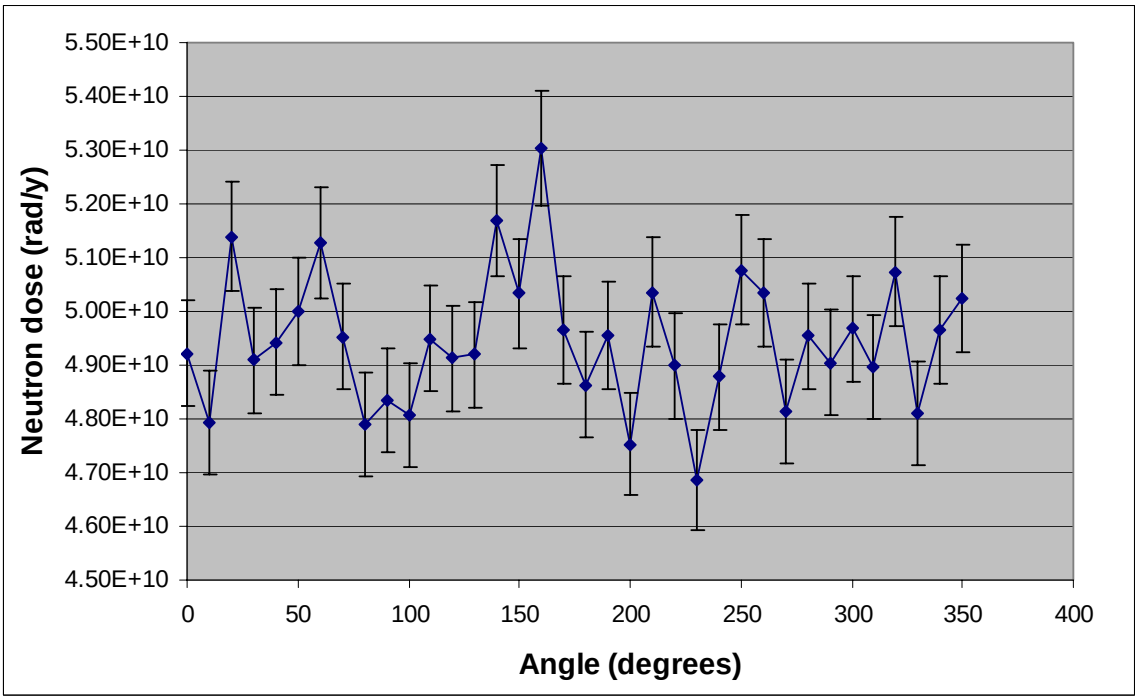

Fig. 4.8. Graph of the neutron dose (rad/y) around the chamber at the plane of the highest neutron dose from Fig. 4.7. Taking into account the error of the simulation, no conclusion can be made about peak doses at any particular angles.

X-ray and debris ablation of the surface of the innermost jets creates a high pressure plasma in the central pocket of the chamber that could cause significant acceleration of the flibe pocket into the wall. The shock from the blast must be adequately mitigated, and the gases must vent properly to allow the pressure near the target to drop. The current tightly packed jet configuration might inhibit venting. Therefore, we propose a possible solution by creating curved venting areas in our jet configuration, as shown in Fig. 4.9 below.

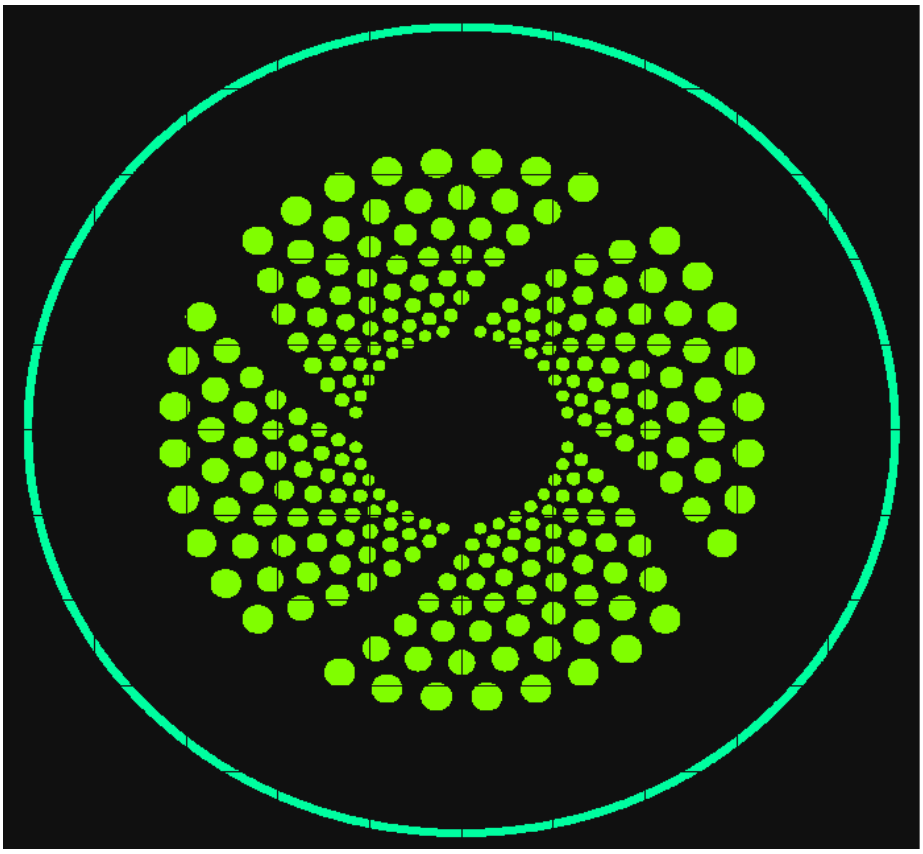

Fig. 4.9. A proposed method to allow the gases to escape from the center area of the chamber during the blast. The curvature of the voids prevents direct exposure of the wall to neutrons, yet still allows the gases to vent.

Including these venting channels should allow the high pressure gas to be released from the area close to the target with less acceleration of the liquid toward the wall. This will have to be simulated to quantify the benefit, likely with TSUNAMI. However, with this new jet array the carbon wall will see a higher neutron dose than with the previous configuration. With this new configuration, we see similar results versus chamber height, but with peak (azimuthally averaged) dose that is ~3× larger. These results are shown in Fig. 4.10.

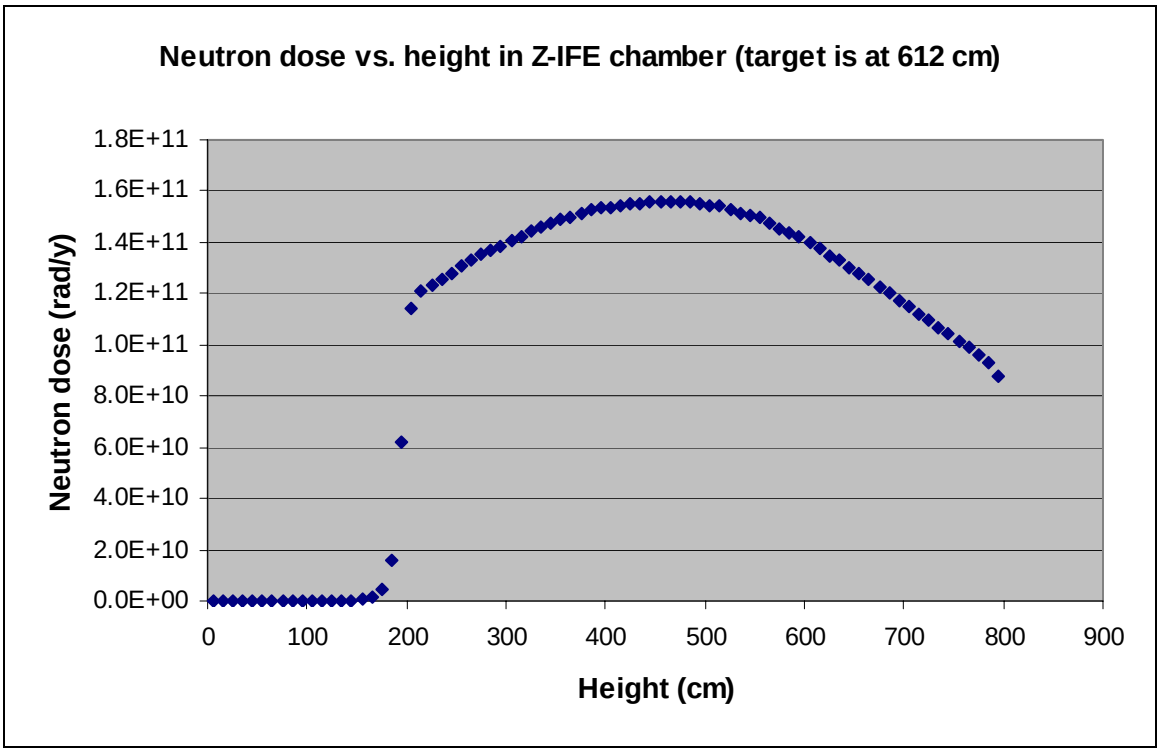

Fig. 4.10. Graph of neutron dose (rad/y) versus the vertical position on the chamber wall. Notice the dose is approximately 3× higher than the case with all flibe jets present.

Since there are four vent channels, it is easier for the neutrons to impact the wall. Originally the dose was fairly uniform across all zones, which is to be expected with symmetric and uniform jet geometries. However, once the voids are put in place, the doses will rise due to neutron scattering. As shown in Fig. 4.11 it is obviously seen that the four venting channels create paths for the neutrons to impact the wall. The peak neutron dose at these points is ~7× larger than for the symmetric, uniform jet case. These dose levels may be unacceptable due to carbon damage issues, so solutions must be engineered. A possible solution would be to put a final jet with a large diameter at the exit point of each of these void regions. This would decrease the neutron dose significantly low to allow for the carbon wall to be used, but still allow for better venting of the gases. The configuration of the jet array to provide good neutron shielding while allowing adequate venting so that the liquid impact on the wall is tolerable is an important design issue that needs more work.

4.6 Conclusions and Recommendations from Neutronics Analyses

Preliminary neutronics calculations and analyses have been performed for the proposed z-pinch IFE power plant. The TART2002 neutron-photon code was used for the analysis of the system. The proposed system is a high-yield, carbon-carbon composite wall, liquid flibe protected inertial fusion energy power plant.

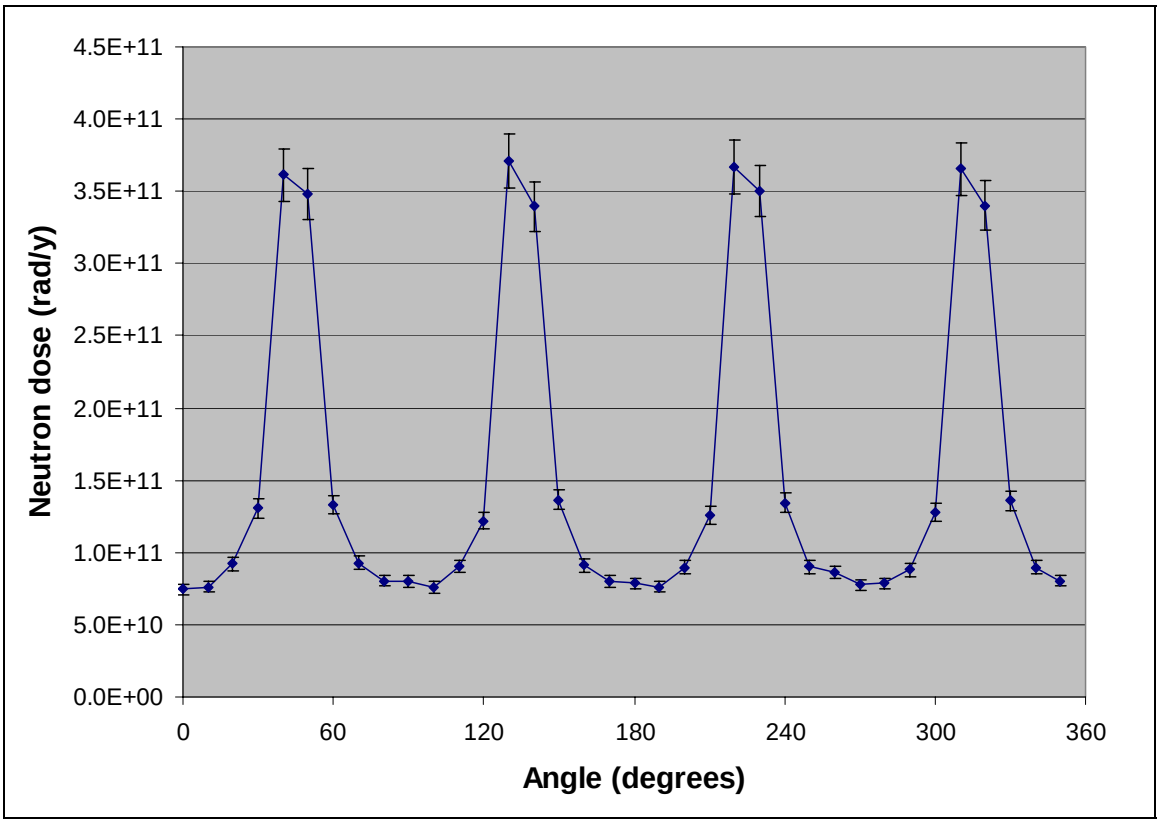

Fig. 4.11. Graph of neutron dose (rad/y) versus angle around the chamber. Notice the peaks due to the four venting channels.

Analysis on the recyclable transmission lines (RTLs) was completed due to the requirement that the lines must be recycled in order to control the amount of activated waste. A neutronics analysis was performed for each element in the periodic table to look for candidate materials that may outperform the current baseline selection for the RTL, iron. Both waste disposal rate and contact dose rate to remote handling equipment was studied for the elements. It was found that iron was an acceptable material when looking at these two tests, however there were also other materials that performed very well. Frozen flibe, if power transmission can be handled, would be a very attractive candidate for the RTLs, as separation from the protecting flibe pocket would not be necessary, and the waste disposal rating and the contact dose rates are very low compared with other materials. Our recommendation is to continue with iron as the baseline material for the RTL. However, possibly in parallel with less effort, frozen flibe RTLs should be studied for use in the power plant.

A study of the chamber liquid protection materials and heat removal fluids was performed. Assuming that 10 times the amount of fluid in the chamber would be needed for a total inventory, we found that the flibe thermal power outside of the chamber would be acceptable. Also, alternate materials were looked at to replace flibe as the working fluid. Liquid lithium and lithium-lead were studied against flibe. It was found that liquid lithium could be used, and should have some minimal effort placed to studying it. However, lithium-lead would require a thickness of nearly 6 meters to provide equal shielding to the flibe. This is entirely too much

fluid to be in our chamber, and would require a much larger chamber and tremendous amounts of fluid. Lithium-lead should not be considered as the liquid coolant/protection for this system.

Significant effort was placed into studying the effects on the chamber wall from the output of the target in this power plant scenario. With such extreme pressures and temperatures inside the system, adequate protection and a very robust wall must be designed in order to contain the blast. At the same time, due to economic concerns, we would like the wall to last the entire lifetime of the power plant. For the example configuration (~1 m effective shielding with a wall radius of 6 m), the radiation damage levels are very low (~10 dpa over 30 years). While other radiation damage effects (e.g., He production in the C/C) remain to be evaluated, we feel that with adequate engineering design a chamber wall that lasts the entire lifetime of the power plant could be designed. We highly recommend the use of a carbon-carbon composite chamber wall if possible, as it would allow for higher chamber temperatures, and therefore higher thermal efficiencies from the power conversion system.

References for Section 4

[1] D. E. Cullen, TART98*: A Coupled Neutron Photon, 3-D, Combinatorial Geometry, Time Dependent, Monte Carlo Transport Code*, UCRL-ID-126455, Rev. 2, Lawrence Livermore National Laboratory (1998).

[2] J. Sanz, ACAB98*: Activation Code for Fusion Applications. User's Manual V4.0*, UCRL-CR-133040, Universidad Nacional de Educacion a Distancia (UNED) and Lawrence Livermore National Laboratory, (1999).

[3] J. F. Latkowski et al., *"Selection of IFE Target Materials from a Safety and Environmental Perspective,"* Nucl. Inst. and Meth. A. 464 (2001) 422-427.

[4] W. R. Meier et al*., "Osiris and SOMBRERO Inertial Confinement Fusion Power Plant Designs,"* W. J. Schafer Associates, Inc., DOE/ER/54100-1, WJSA-92-01 (1992).

[5] R. W. Moir, R. L. Bieri, X. M. Chen, T. J. Dolan, M. A. Hoffman, P. A. House, R. L. Leber, J. D. Lee, Y. T. Lee, J. C. Liu, G. R. Longhurst, W. R. Meier, P. F. Peterson, R. W. Petzoldt, V. E. Schrock, M. T. Tobin, W. H. Williams, *"HYLIFE-II: A Molten Salt Inertial Fusion Energy Power Plant Design – Final Report,"* Fusion Technol., 25 (1994) 5-25.

[6] G. Rochau, ZPF Project Memorandum, "Suggested New Baseline RTL Design," October, 21, 2002.

5. Findings and Recommendations

In this document we report LLNL's progress in the conceptual design of a Z-IFE power plant. Given the very short timeframe for this study (3 months), much of the work is investigative by nature. A great deal of additional work will be needed to develop a robust design of the type suggested. Nevertheless, this work adds significantly to the Z-IFE knowledge base and, more importantly, helps guide future work in directions that may offer considerable advantages. Specifically, we seek to broaden the Z-IFE design space by offering alternative perspectives on several key components and parameters: the fusion yield per target, the choice of chamber material, and the choice of RTL material. Our analysis on liquid motion and chamber response identifies multiple issues that need to be addressed in future work. Our specific findings include the following:

- Since the cost of targets is likely to be very important, significant economic advantages are possible through a move to higher fusion yields per target and a reduction in the number of independently operating target chambers.

- The use of a carbon-carbon composite wall offers some interesting advantages over a ferritic steel wall. In particular, the carbon wall would be able to attain higher temperatures, and thus, higher thermal efficiencies. Also, a carbon wall would enable the use of an "oxidizing" (fluoridizing) molten salt, which would simplify RTL reprocessing and tritium handling.

- When coated with a silicon layer and heated during fabrication, a carbon composite wall may be able to withstand corrosion from reduced flibe and have a very low tritium permeation.

- With approximately 1 m of flibe protection, a carbon composite wall only would receive at most 10 dpa in 30 full-power years of operation (in most locations, the damage rate is considerably lower than 10 dpa). Thus, it is likely to be a lifetime component and experience only minimal contraction and/or swelling.

- Peak stresses in the wall appear to be acceptable for 3 GJ yields, but methods for stress reduction must be implemented for 20 GJ yields. This might be accomplished through a combination of several modifications: increasing the wall thickness, increasing the chamber volume, and/or thickening the liquid protection.

- The momentum imparted to the liquid jets is sufficient to make wall erosion a concern that must be addressed and/or reduced in future work.

- From the material recycling and waste management perspectives, there are many materials that would have acceptable performance as an RTL material. Options should be left open at this time, and other factors such as cost, flibe chemistry, compatibility with carbon, ability to fabricate and electrical resistivity (of the resulting plasma) must be considered.

Appendix A

Mathcad Systems Model

Preliminary Z-IFE Systems Model

Target performance info from Olson presentations

$i := 1, 2 .. 3$

Current $I_i :=$	Xray energy, MJ $Ex_i :=$	Absorbed , MJ $Ea_i :=$	Yield, MJ $Y_i :=$
54	12	2.4	530
86	30	6	3000
95	37	7.2	4400

Target Gain

$Gp_i := \frac{Y_i}{Ex_i}$ Define gain in terms of x-ray energy produced by z-pinch

$Gp_i =$

44.2
100.0
118.9

Fit thru two high yield point gives a pretty good result at lowest point. This scaling (0.825) is stronger than Perkins finds for direct drive lasers (0.6).

$G(E) := 100 \cdot \left(\frac{E}{30}\right)^{0.825}$

$G(12) = 47.0$

$G(30) = 100.0$

$G(37) = 118.9$

$Ed := 0, 1 .. 100$

Target gain vs x-ray energy

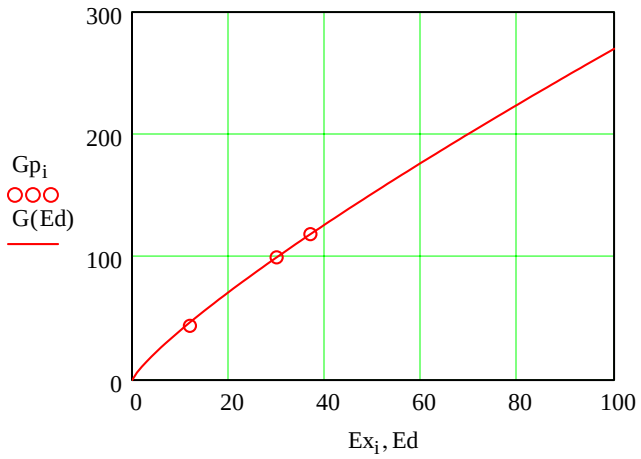

Target yield, MJ

$Y(E) := G(E) \cdot E$ $\quad Y(12) = 563$ Scaling is slightly high (+6%) at 12 MJ

$Y(30) = 3000$

$Y(37) = 4399$

Define a reference point for COE comparison

$Eo := 25$ $\quad Y(Eo) = 2.151 \times 10^{3}$

$Ed := 10, 12 .. 85$

Yield vs driver x-ray energy
Calculated point shown

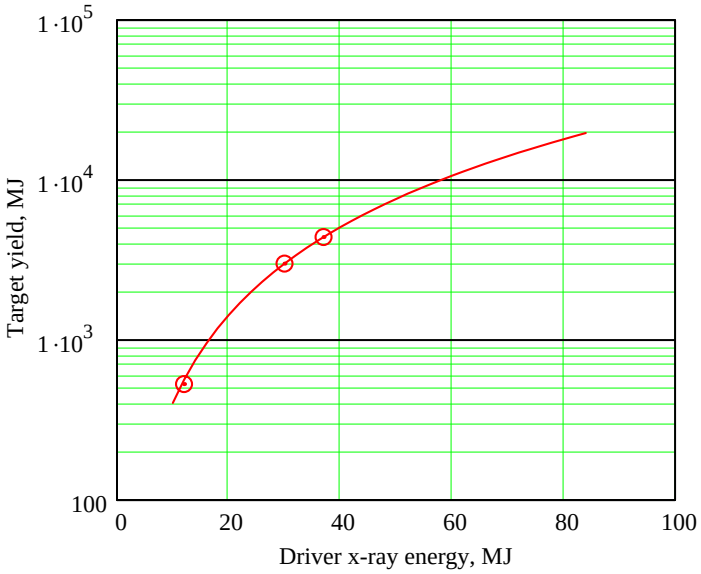

Power Balance:

RR = rep-rate, HZ

Set driver efficiency and power plant thermal-to-electric conversion efficiency

$\eta d := 0.15$ $\quad \eta t := 0.5$

Thermal power per unit, MW (system energy multiplication factor = 1.14 re Latkowski)

$Ptu(E, RR) := E \cdot G(E) \cdot RR \cdot 1.14$ $\quad Ptu(Eo, 0.1) = 245.2$

$G(Eo) = 86$

$Y(Eo) = 2151$

Gross electric power per unti

$Pgu(E, RR) := Ptu(E, RR) \cdot \eta t$ $\quad Pgu(Eo, 0.1) = 122.6$

Driver power consumption per unit

$$Pdu(E, RR) := \frac{E \cdot RR}{\eta d} \qquad Pdu(Eo, 0.1) = 16.7$$

Total net power for Nu units

$$Pnet(E, RR, Nu) := 0.96 \cdot Pgu(E, RR) \cdot Nu - \frac{E \cdot RR \cdot Nu}{\eta d}$$

Includes 4% reduction for in plant auxiliary power requirements

Eo = 25 MJ, RR = 0.1 Hz, Nu = 10 gives ~ 1GWe net power

$$Pnet(Eo, 0.1, 10) = 1010$$

Guestimate Cost Scaling

Assume 10 drivers account for 10% of plant cost for 10 unit plant. Cost scale linearly with driver (x-ray) energy and number of units

$$Cd(E, Nu) := 0.1 \cdot \frac{E}{Eo} \cdot \frac{Nu}{10} \qquad Cd(Eo, 10) = 0.1$$

Assume chambers are also 10% of cost of 10 unit plant. Radius scales as Y^1/3 (fix energy density), cost as R^2, so costs go as Y^2/3.

$$Cch(E, RR, Nu) := 0.1 \cdot \left(\frac{Y(E)}{Y(Eo)} \right)^{0.67} \cdot \frac{Nu}{10} \qquad Eo = 25 \qquad Y(Eo) = 2151$$

Assume power conversion system is 60% of cost of 10 unit plant, scales as unit power to the 0.8 (each unit has its own

$$Cpp(E, RR, Nu) := 0.6 \left(\frac{Pgu(E, RR) \cdot Nu}{Pgu(Eo, 0.1) \cdot 10} \right)^{0.8} \qquad Pgu(Eo, 0.1) = 122.6$$

Assume target factor is 20% of plant cost and scale with production rate to the 0.7

$$Ctf(RR, Nu) := 0.2 \cdot \left(\frac{RR \cdot Nu}{0.1 \cdot 10} \right)^{0.7}$$

Total (normalized) cost

$$Ctot(E, RR, Nu) := Cd(E, Nu) + Cch(E, RR, Nu) + Cpp(E, RR, Nu) + Ctf(RR, Nu)$$

$$Ctot(Eo, 0.1, 10) = 1$$

Normalize cost of electricity

$$COE(E, RR, Nu) := \frac{Ctot(E, RR, Nu)}{Pnet(E, RR, Nu)} \cdot \frac{Pnet(Eo, 0.1, 10)}{Ctot(Eo, 0.1, 10)}$$

Calculate rep-rate for fixed net electric power $TOL := 0.0001$

$Pfix := Pnet(Eo, 0.1, 10)$ set fixed at net power for 25 MJ, 0.1 Hz, 10 Units

$Pfix = 1010$

$RRgv := 0.1$ guess value

$RRfp(E, Nu) := root(Pnet(E, RRgv, Nu) - Pfix, RRgv)$ Rep-rate for fixed power

$RRfp(Eo, 10) = 0.1$ checks

Driver energy for fixed net power and fixed 0.1 Hz per unit for different number of units, Nu:

$Egv := 10$

$Efprr(Nu) := root(RRfp(Egv, Nu) - 0.1, Egv)$

Define energies for 10, 5 and 1 units:

$E10 := Efprr(10)$ $E10 = 25.0$ $Y(E10) = 2150$

$E5 := Efprr(5)$ $E5 = 35.7$ $Y(E5) = 4128$

$E1 := Efprr(1)$ $E1 = 83.6$ $Y(E1) = 19464$

COEs for 10, 5 and 1 unit all at 0.1 Hz per unit

$COE10 := COE(Efprr(10), 0.1, 10)$ $COE10 = 1.000$ checks

$COE5 := COE(Efprr(5), 0.1, 5)$ $COE5 = 0.852$

$COE1 := COE(Efprr(1), 0.1, 1)$ $COE1 = 0.672$

Normalized captial cost vs driver x-ray energy
1 GWe net power, 10 unit plant

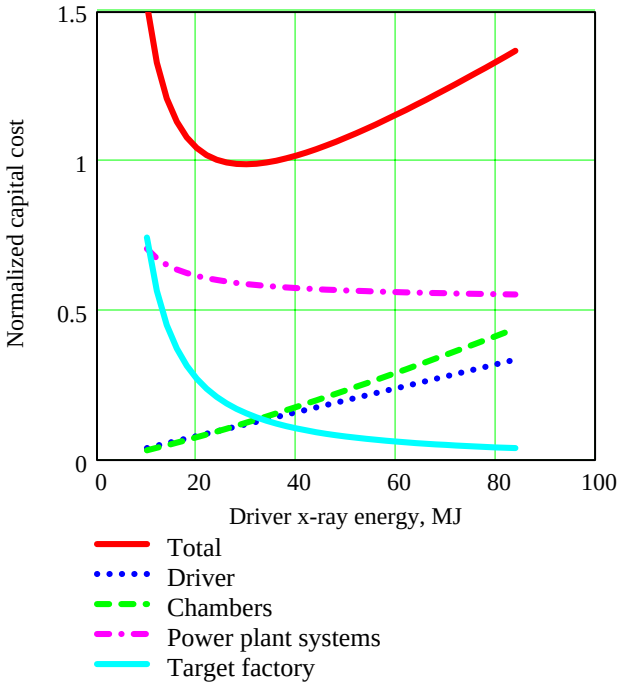

Normalized COE vs. driver x-ray energy
10, 5 and 1 unit plants, 1 GWe total net power
Circles correspond to chamber rep-rate of 0.1 Hz

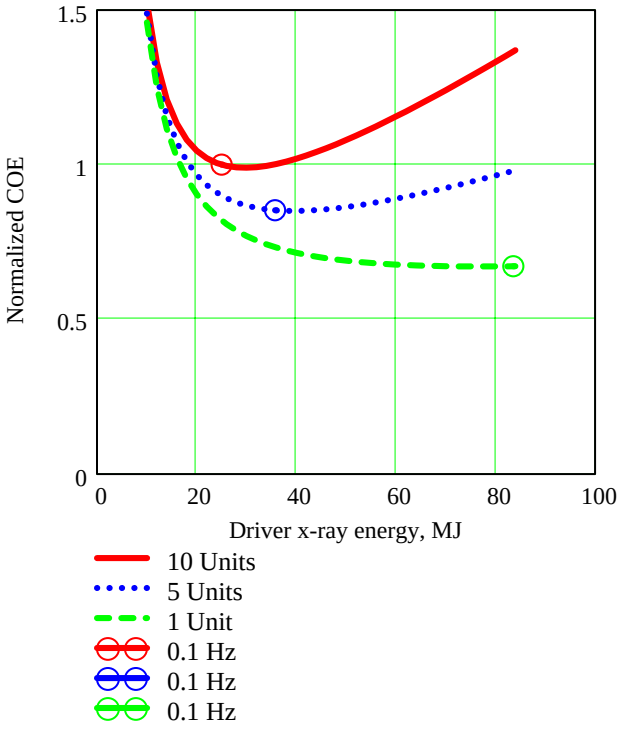

Normalized COE vs. chamber rep-rate
10, 5 and 1 units per plants, 1 GWe total net power

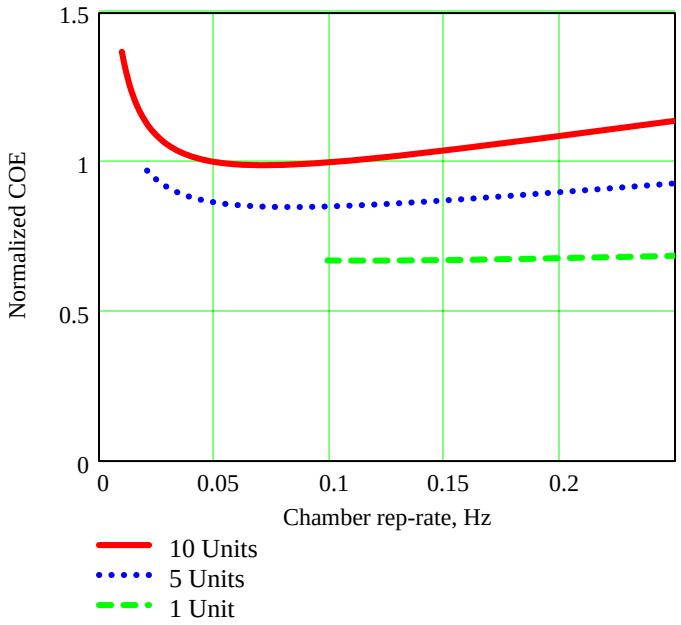

With the assumed scalings, higher yields and lower chamber rep-rates, e.g., down to 0.05 Hz or 20 sec between pulses, have little impact on COE for the 5 and 10 unit plants. For the 1 unit plant, we limit yield to 20 MJ, which corresponds to ~0.1 Hz for 1 GWe.

Optimal Points

10 units		5 units	1 unit
$Y(30) = 3.00 \times 10^3$	MJ	$Y(40) = 5.07 \times 10^3$	$Y(80) = 1.797 \times 10^4$
$RRfp(30,10) = 0.07$	Hz	$RRfp(40,5) = 0.081$	$RRfp(80,1) = 0.109$
$\frac{1}{RRfp(30,10)} = 14.3$	sec	$\frac{1}{RRfp(40,5)} = 12.4$	$\frac{1}{RRfp(80,1)} = 9.2$
$COE(30, RRfp(30,10), 10) = 0.99$		$COE(40, RRfp(40,5), 5) = 0.85$	$COE(80, RRfp(80,1), 1) = 0.671$

Appendix B

Mathcad First Wall Stress Model

Shock Mitigation by Liquid Jets and Peak First Wall Stress

Liquid Ablation

Target yield [J]

$Yo \equiv 3 \cdot 10^{9}$

Mass density of flibe [kg / m^3]

$\rho \equiv 2000$

Target yield fractions:

x-rays debris neutrons

$\xi \equiv 0.15 \quad \beta \equiv 0.15 \quad \nu \equiv 1 - (\xi + \beta)$

Pocket radius [m]	Pocket height [m]	Shielding density	Shielding thickness [m]
$Ro \equiv 1.5$	$Ho \equiv 4$	$\sigma o \equiv 0.33$	$\Delta Ro \equiv 3$

Aerial density of shielding [kg / m^2] This is the amount of shielding mass for each unit of target facing surface area. The target facing surface area is the area exposed to x-rays and target debris and is, hence, equal to the ablation area defined below.

$$\mu(R, \Delta R, \sigma) \equiv \frac{\sigma \cdot \rho \cdot \left[(R + \Delta R)^2 - R^2 \right]}{2 \cdot R}$$

Ablation area [m^2]

$A(R, H) \equiv 2 \cdot \pi \cdot R \cdot H$

The depth to which liquid will be ablated is dependent upon the X-Ray fluence to target facing liquid surfaces. Fig. 4-4 in the HYLIFE-II Progress Report gives data for this relationship. The following numbers are pulled from that plot.

x-ray fluence [J / m^2] and corresponding ablation depth [m] data

$$f \equiv \begin{pmatrix} 7 \cdot 10^{3} \\ 9 \cdot 10^{3} \\ 1.4 \cdot 10^{4} \\ 3.5 \cdot 10^{4} \\ 7 \cdot 10^{5} \\ 2 \cdot 10^{8} \end{pmatrix} \qquad d \equiv \begin{pmatrix} 10^{-9} \\ 10^{-8} \\ 10^{-7} \\ 10^{-6} \\ 10^{-5} \\ 10^{-4} \end{pmatrix}$$

$i := 0, 1 .. \text{rows}(d) - 1$

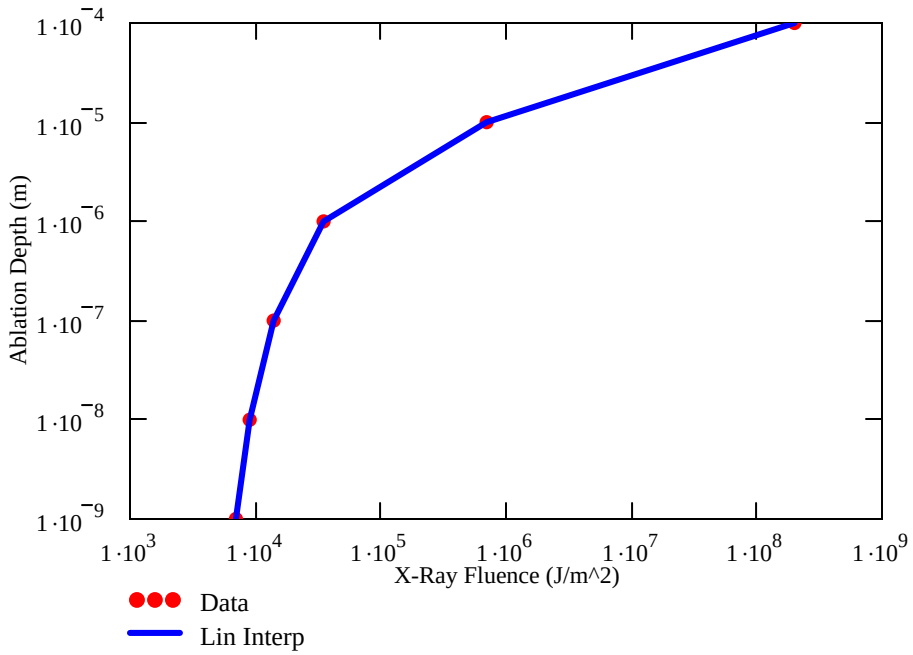

Peak x-ray fluence to ablation surfaces [J / m^2].

$$\phi(Y,R) \equiv \frac{\xi \cdot Y}{4 \cdot \pi \cdot R^2}$$

Solid angle fraction subtended by ablated area

$$\kappa(R,H) \equiv \cos\left(\operatorname{atan}\left(\frac{2 \cdot R}{H}\right)\right)$$

Peak ablation depth [m]

$$\delta(Y,R) \equiv \text{linterp}(f, d, \phi(Y,R))$$

Ablated mass [kg]. This is a conservative estimate because the peak ablation depth is applied to all target facing surfaces. In reality, liquid surfaces off the target plane will experience x-ray deposition that is off normal resulting in lesser ablation depths. Also, these surfaces will be a greater distance from the target and fluences will be reduced.

$$m_p(Y,R,H) \equiv \delta(Y,R) \cdot A(R,H) \cdot \rho$$

$$m_p(Yo, Ro, Ho) = 1.272$$

Dissociation energy of flibe [J / kg]. This is the amount of energy per kilogram needed to raise the liquid to boiling, perform the phase change to vapor, and dissociate the molecules completely.

$\varepsilon_d \equiv 2.1 \cdot 10$

Ionization energy of flibe [J / kg]. This is the energy needed to strip the electrons from the dissociated molecules to create a plasma.

$$\varepsilon_i \equiv 7.57 \cdot 10^7$$

Kinetic energy of ablated mass [J]

$$E(Y,R,H) \equiv \left[(\xi + \beta) \cdot Y \cdot \kappa(R,H) - (\varepsilon_d + \varepsilon_i) \cdot m_p(Y,R,H) \right]$$

Specific ablation impulse [Pa x s]

$$I(Y,R,H) \equiv \frac{\sqrt{2 \cdot m_p(Y,R,H) \cdot E(Y,R,H)}}{A(R,H)}$$

Resulting liquid speed toward wall [m / s]

$$v_a(Y,R,H,\Delta R,\sigma) \equiv \frac{I(Y,R,H)}{\mu(R,\Delta R,\sigma)}$$

$$v_a(Yo,Ro,Ho,\Delta Ro,\sigma o) = 0.261$$

Pocket Pressurization and Venting

Pocket volume [m^3]

$$V(R,H) \equiv \pi \cdot R^2 \cdot H$$

Dissociation energy for flibe at 5000 K [J / kg]. The HYLIFE-II progress report assumes this temperature is reached before venting begins.

$$\varepsilon_c \equiv 7.3 \cdot 10^6$$

Specific heat ratio of flibe [Cp / Cv]

$$\gamma \equiv 1.2$$

Gas constant [J / mol / K]

$$R_g \equiv 8.31$$

Boltzmann constant [J / K]

$$k \equiv 1.380658 \cdot 10^{-23}$$

Venting area fraction

$$\eta o \equiv 0.4$$

Molecular mass of LiF [kg / mol]

$$M_L \equiv 0.02594$$

Molecular mass of BeF2 [kg / mol]

$$M_B \equiv 0.047$$

Average molecular mass of flibe [kg / mol]

$$M_{flibe} \equiv \frac{2 \cdot M_L + M_B}{3}$$

Avogadro's number

$$N_a \equiv 6.0221367 \cdot 10^{23}$$

Vapor temperature [K]

$$T \equiv 5000$$

Number of BeF2 molecules that can be vaporized by target to temperature T [K]

$$n_B(Y) \equiv \frac{(\xi + \beta)\cdot Y}{\frac{\varepsilon_c}{N_a}\cdot(2\cdot M_L + M_B) + 13\cdot k\cdot T}$$

Number of LiF molecules vaporized to temperature T

$$n_L(Y) \equiv 2\cdot n_B(Y)$$

Mass of BeF2 molecules [kg]

$$m_B(Y) \equiv \frac{n_B(Y)}{N_a}\cdot M_B$$

Mass of LiF molecules [kg]

$$m_L(Y) \equiv \frac{n_L(Y)}{N_a}\cdot M_L$$

Total mass of flibe vapor [kg]

$$m_v(Y) \equiv \left(m_B(Y) + m_L(Y)\right)$$

$$m_v(Yo) = 70.502$$

Energy in vaporized mass contributing to pressure [J]

$$E_g(Y) \equiv (\xi + \beta)\cdot Y\cdot\left[1 - \frac{m_v(Y)\cdot\varepsilon_c}{m_v(Y)\cdot\varepsilon_c + \left(\frac{7}{2}\cdot n_L(Y) + 6\cdot n_B(Y)\right)\cdot k\cdot T}\right]$$

Initial pocket pressure [Pa]

$$P_o(Y,R,H) \equiv \frac{(\gamma - 1)\cdot E_g(Y)}{V(R,H)}$$

$$P_o(Yo,Ro,Ho) = 2.726\times 10^6$$

Vaporized liquid sound speed [m / s]

$$C_g \equiv \sqrt{\frac{\gamma\cdot R_g\cdot T}{M_{flibe}}}$$

Venting time constant [s]

$$\tau(R,H,\eta) \equiv \frac{V(R,H)}{C_g\cdot\eta\cdot A(R,H)}$$

Resulting liquid speed toward wall [m / s]

$$v_v(Y,R,H,\Delta R,\sigma,\eta) \equiv \frac{P_o(Y,R,H)\cdot\tau(R,H,\eta)}{\mu(R,\Delta R,\sigma)}$$

$$v_v(Yo,Ro,Ho,\Delta Ro,\sigma o,\eta o) = 1.049$$

Neutron Isochoric Heating

Gruneisen parameter for flibe

$\Gamma \equiv 0.98$

Liquid sound speed of flibe [m / s]

$C_l \equiv 3250$

Energy dissipation fraction

$\lambda \equiv 0.3$

Mass of liquid flibe [kg].

$m_l(R, \Delta R, H, \sigma) \equiv \pi \cdot \rho \cdot \sigma \cdot \left(\Delta R^2 + 2 \cdot \Delta R \cdot R\right) \cdot H$

Resulting liquid speed toward wall [m / s]

$$v_n(Y, R, H, \Delta R, \sigma) \equiv \frac{\nu \cdot Y \cdot \Gamma \cdot \lambda \cdot \kappa(R, H)}{C_l \cdot m_l(R, \Delta R, H, \sigma)}$$

$$v_n(Yo, Ro, Ho, \Delta Ro, \sigma o) = 1.018$$

Total Liquid Speed

Total resulting liquid speed [m / s]

$$v(Y, R, H, \Delta R, \sigma, \eta) \equiv v_a(Y, R, H, \Delta R, \sigma) + v_v(Y, R, H, \Delta R, \sigma, \eta) + v_n(Y, R, H, \Delta R, \sigma)$$

$$v(Yo, Ro, Ho, \Delta Ro, \sigma o, \eta o) = 2.328$$

Stresses in the FSW

Radius of chamber [m]

$Rco := 6$

Height of chamber [m]

$Hco := 6$

FSW density [kg/m^3]

$\rho_{FSW} \equiv 7800$

Elastic modulus [Pa]

$G \equiv 190 \cdot 10^9$

Poisson's Ratio

$\omega \equiv 0.3$

Thickness of chamber wall [m]

$to \equiv 0.05$

Peak FSW stress [Pa]

$$\sigma(Y, R, H, \Delta R, \sigma, \eta, t, Rc, Hc) \equiv \frac{v(Y, R, H, \Delta R, \sigma, \eta) \cdot m_l(R, \Delta R, H, \sigma)}{t \cdot A(Rc, Hc)} \cdot \sqrt{\frac{G}{2 \cdot \rho_{FSW}\left(1 - \omega^2\right)}}$$

$$\sigma(Yo, Ro, Ho, \Delta Ro, \sigma o, \eta o, to, Rco, Hco) = 1.124 \times 10^8$$

Parameter Variation Impact on Liquid Speed and Peak FSW Stress

Liquid speed

$P := 0.5, 0.6 .. 2$

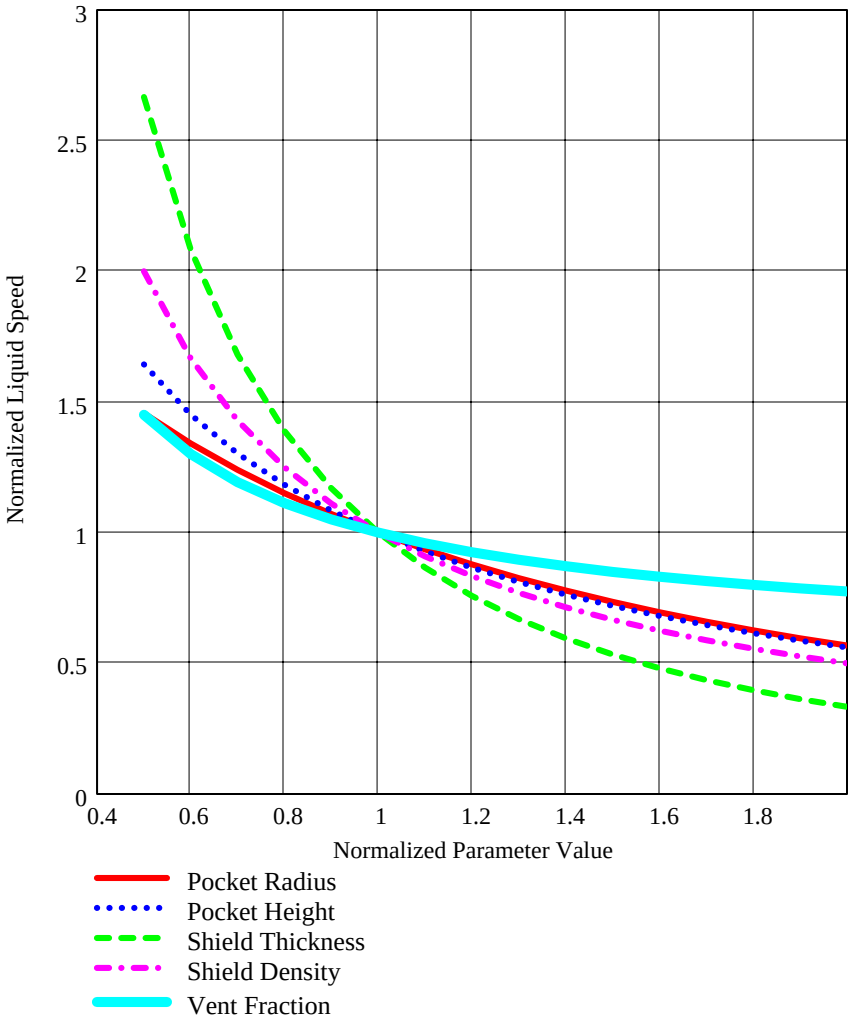

Peak FSW stress normalized to result for:

Ro = 1.5 Ho = 4 to = 0.05 Yo = 3×10^9

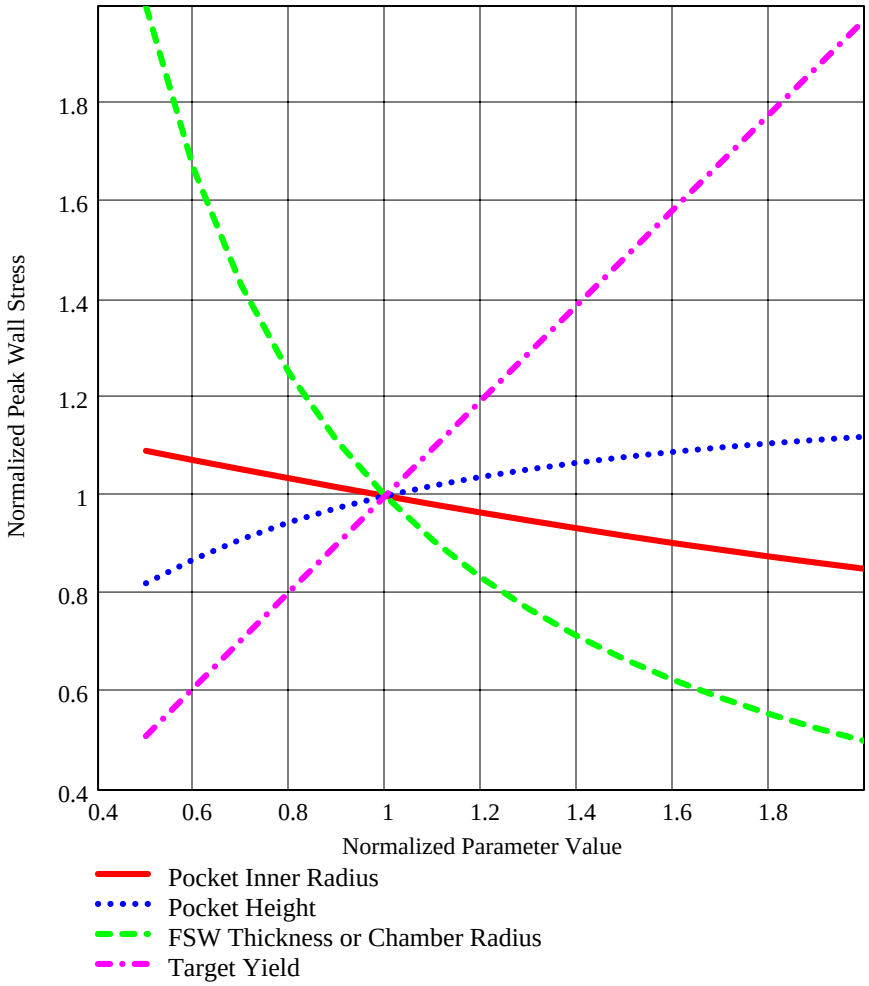

Appendix C. Miscellaneous Calculations and Considerations

In this Appendix we discuss a variety of miscellaneous topics that were considered as part of our investigation of the Z-IFE chamber and power plant. These include:

C.1 Vessel Material Options and Tritium Containment
C.2 Cost and Development of the Vessel
C.3 Why Have 10 to 20 Torr of Inert Gas in the Chamber?
C.4 Vapor Pressure of Flibe and Vaporization (Condensation) Rates
C.5 Alternatives to Tungsten Wires
C.6 Alternatives to Steel RTL
C.7 Flibe Cost Estimate
C.8 Flibe Volume Estimate

C.1 Vessel Material Options and Tritium Containment

The vessel is assumed to be made of either ferritic steel or carbon composites. The advantage of steel is it is compatible with flibe in its reduced state up to the point it looses its strength at about 550 to 600 °C, it is low cost and fabricable. Its disadvantage is the temperature limitation. The advantage of carbon composites is the temperature can go to 1000 °C where Brayton cycles and hydrogen thermochemical cycles are possible and is chemically compatible with flibe including TF [1]. There are a number of disadvantages. High cost, difficulty of fabrication, joining, sealing, are problems that need solutions.

The ferritic steel example shown below (Fig. C-1) is similar to that of HYLIFE-I except in its tritium containment. HYLIFE-I used lithium. Tritium permeation was not a problem because the lithium held tritium tightly as a hydride. With flibe in its reduced state tritium will be very diffusive and easily permeate through walls. We show double walls for tritium containment. The insulation region would have an inert gas that is processed for tritium. The lower temperature steel walls will have reduced permeation aid containment.

The carbon composite example shown below (Fig. C-2) can operate over 1000 °C. We suggest a silicon layer be applied during fabrication. Then the temperature would be raised over the silicon melt of 1400 °C where the Si reacts with C to form a layer of SiC. This layer holds the promise of hermetically sealing the chamber including greatly reduced tritium permeation. This same method might be successful for flat plate heat exchangers compatible with flibe and forming a tritium barrier. If the silicon and silicon carbide are in poor contact with the flibe, the combination might be compatible with flibe in its fluoridized state where tritium is largely in the form of TF. The reason is corrosion would take place largely by gas phase transport and hence through the not very porous media would be severely rate limited.

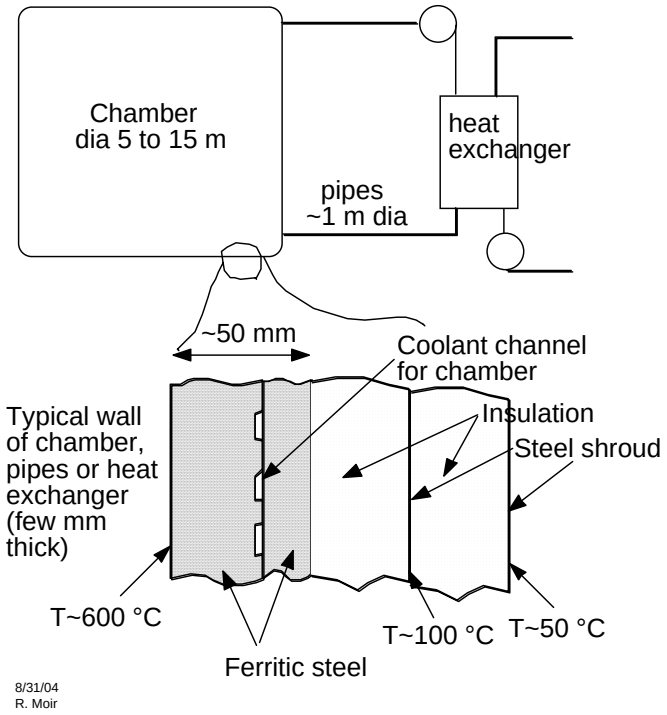

Fig. C-1. Ferritic steel chamber, pipe and heat exchanger walls.

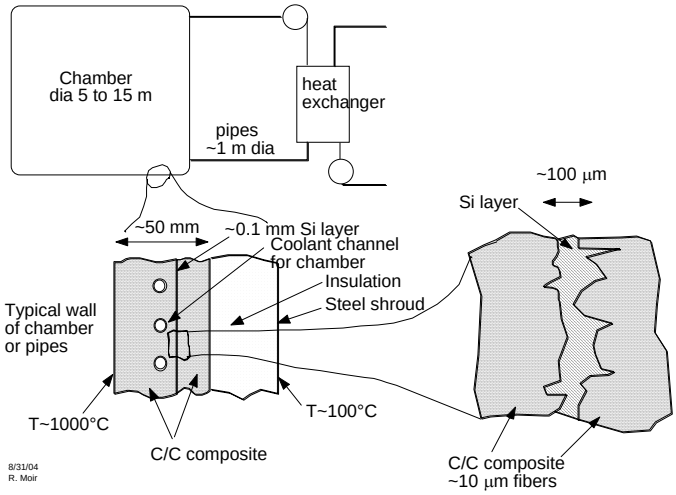

Fig. C-2. Carbon-composite chamber, pipe and heat exchanger walls.

C.2 Cost and Development of the Vessel

The HYLIFE-II vessel was assumed to be made of 304 SS because the nickel would make corrosion by TF less. The present suggestion is to use ferritic steel up to 550 or 600 °C and use carbon composites at ~1000°C. Some useful scaling parameters based on P. House [2] are given in Table C-1.

Table C-1 Vessel Parameters from HYLIFE-II

Electric power	1 GWe case	2 GWe case
Radius of vessel	3.5 m	4.75 m
Wall thickness	50 mm	50 mm?
Yield	350 MJ	600 MJ
Cost 93$	30 M$	55 M$
Mass	270 Ton	530 Ton
Unit costs	110 $/kg	104 $/kg

The cost of ferritic steel should be lower than that of 304 SS on a $/kg of fabricated parts and more for carbon composites. At the same stress the carbon composites should be about 4 times lower mass. A carbon composite vessel at the same cost can cost about 110 X 3.9=$430/kg. At higher yield the vessel grows in size. Also at higher power the vessel grows some. Scaling follows from:

$\sigma = \frac{P\tau}{T}\sqrt{\frac{E}{2\rho(1-\nu^2)}}$ = wall stress, where P is pressure, τ is impact time, T is the wall thickness

$P\tau \propto Yield/4\pi r^2$ = specific impulse, where Yield is the target yield

$r^2 T \propto Yield$ at constant stress

cost $\propto r^2 T \propto Yield$

Also the cost $\propto \frac{\rho}{\sigma} \cdot$ material cost$(\frac{\$}{kg})$

Carbon composites can cost several times more in $/kg than steel at the same stress.

For carbon composite construction to be practical we need to develop methods of hermetically sealing the porous C/C perhaps with chemical vapor deposition of carbon followed by silicon layering that is reacted at 1400 °C for form a SiC layer. We need to develop joining methods, perhaps bolted joints with “O-ring” seals. We need to develop methods to repair parts. We need pipes and heat exchanges to be developed of C/C. Finally, the cost must be in the range of $400/kg to be economical, at least not several or ten times that.

C.3 Why Have 10 to 20 Torr of Inert Gas in the Chamber?

Inert gas, Xe or Kr is often suggested to protect walls from x rays. The gas absorbs the x rays and re-emits over a longer time. Liquid jets protect the walls from neutrons and at the same time from x rays. The inert gas is a non-condensable gas that interferes with condensation. We should avoid inert gas or minimize it. If we have no inert gas, avoiding the rush of gas up the transmission lines should make keeping them clean easier. Fast acting shut off valves will be needed.

C.4 Vapor Pressure of Flibe and Vaporization (Condensation) Rates

The vapor pressure and evaporation rates are calculated from the following equations and plotted in Fig. C-3 and C-4:

$$P(\text{Pa}) = e^{A-B/T}$$

$$J = \frac{n\bar{v}}{4} = \frac{p}{(2\pi mkT)^{0.5}} = CT^{-0.5}e^{(A-B/T)} \quad \#/\text{m}^2\text{s}$$

Here, A=26.59, B=25,390, and C=3.828x10^{23} for BeF_2 evaporation. The flibe vapor pressure used was $\log_{10} P_{torr} = 9.424 - 11026.208/T(K)$ and was converted to pascals [3,4]. This latest estimate of vapor pressure and therefore evaporation rates are about a factor of three lower than previous estimates in the 500 °C range as can be seen in Fig. C-3. At 1000 °C (not shown) they are about the same.

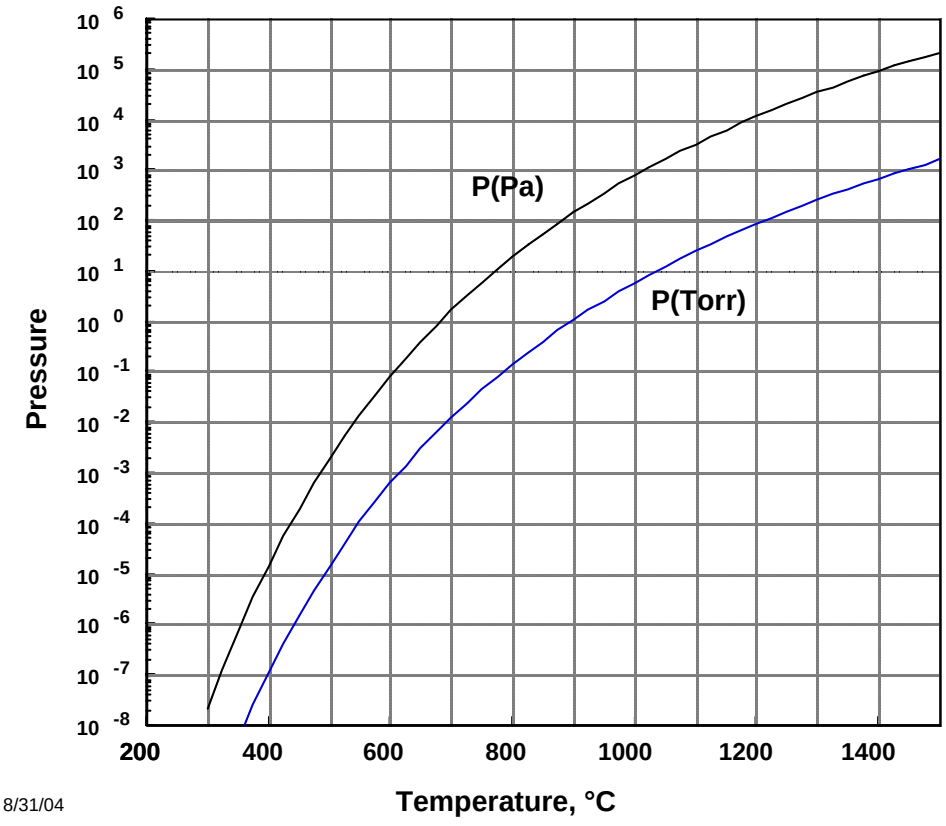

Fig. C-3. Flibe vapor pressure in Pa and Torr (= Pa/133.3).

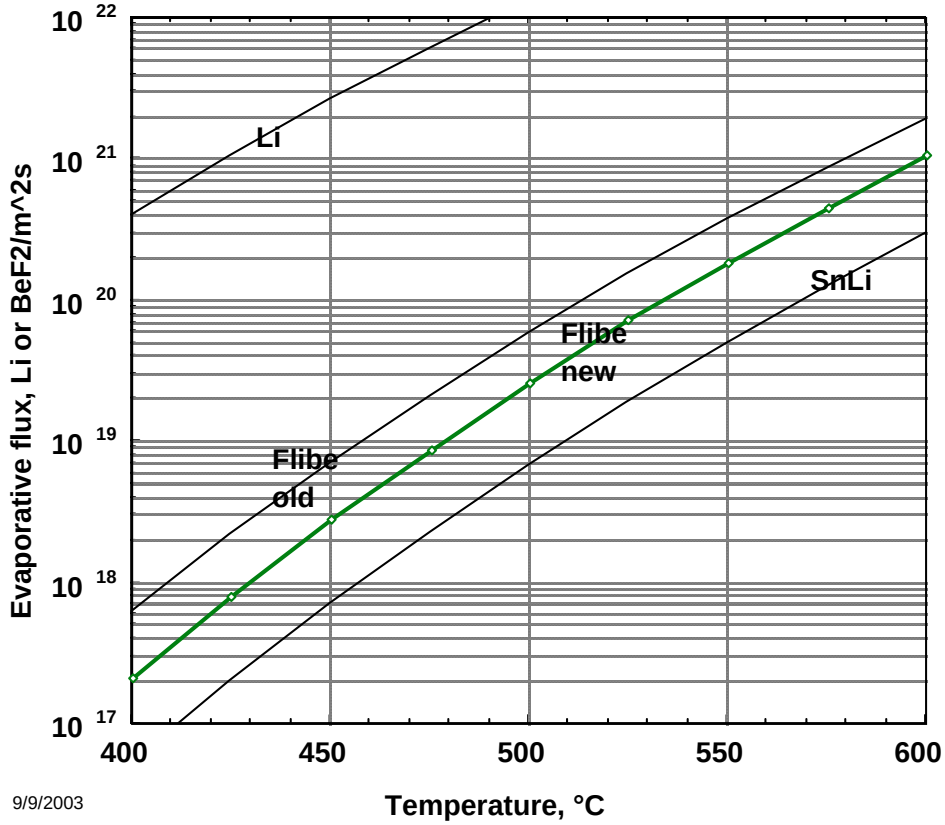

Fig. C-4. Evaporation (and condensation) rates into vacuum for candidate liquids.

At equilibrium $J_{evaporation} = J_{condensation}$.

C.5 Alternatives to Tungsten Wires

The problem with tungsten wires is recovery from flibe. Tungsten will form finely divided solids in the salt. Alternatively, lead or bismuth or mercury could be considered. Maybe other examples would work. Lead and bismuth are liquids and can be recovered by centrifuging and then flowing. The problem is attack of metal surfaces. Also Bi results in Po, which is a waste disposal problem. Mercury is a solid at low temperatures but a vapor under operating conditions and evaporative separation is straightforward. The mercury can be recovered with ppm levels remaining. Corrosion at these low levels might be completely manageable. Safety under accident conditions of course must be weighed.

C.6 Alternatives to Steel RTL

In the HYLIFE-CT we considered frozen flibe for a similar double conical transmission line of about 2.5-m length. The inner surface would be coated with a conductor, for example lead or mercury. Recovery seems straightforward as opposed to recovery and reuse of steel.

C.7 Flibe Cost Estimate

When large quantities of flibe are contemplated one wonders if the cost is an issue. This subject was discussed in two memos and a letter quote from Brush-Wellman for 100 ton quantities of BeF_2 with the conclusions summarized here [5-7]:

42 \$/kg (1994\$) for first of a kind use or 52.5 \$/kg (2004\$)

34 \$/kg (1994\$) for 10^{th} of a kind use or 42.5 \$/kg (2004\$)

where we use 1.25 to convert from 1994 to 2004 dollars with an estimate of 2.5 % per year in recent years.

Flibe delivered to a plant would be considered more like a fuel charge than as capital so that the indirect costs associated with it would be much less than for capital items that can easily be 100% add-on. The cost of make up ^{6}Li was found to be insignificant (1/3 M\$/yr for a typical 1 GWe power plant). HYLIFE-II calls for use of about 1250 m^3 of flibe or 2500 Mg (tonnes). Our cost estimate for flibe is \$34/kg (1994\$) or \$71 M direct, which contributes 2.9% to the cost of electricity (COE) of 4.4 ¢/kWh. A 10% change in the estimated cost of flibe would give a 0.3% change in COE. The increasing concerns over health effects due to use of beryllium warrant being cautious about the validity of these cost estimates.

C.8 Flibe Volume Estimate

Most of the flibe at any one time is in the piping system flowing to and from pumps, vacuum disengagers, and heat exchangers. Less than 10% is in the chamber at any one time. It follows that the volume will be insensitive to yield. In HYLIFE-II the volume estimated was approximately 1200 m^3 using the following scaling equation

$$V_{flibe}(m^3) = 5.6 \cdot P_{thermal}(MW)^{0.5} + 310 \cdot \frac{P_{thermal}(MW)}{1100\,MW}$$

The idea is that many of the components scale with square root of power (first term) meaning larger units utilize flibe better, but that the heat exchangers will be built in approximately 1100 MW_{th} size and higher power will add more units and require more flibe (second term).

References for Appendix C

1. G. Fukuda and P. Peterson, "Carbon in fluoride systems" UN Berkeley Dept of Nuclear Engineering note, 8/25/2004.
2. P.A. House, "HYLIFE-II reactor chamber design refinements," Fusion Technology **26** (1994) 1178-1195.
3. D.R. Olander, G.T. Fukuda, and C.F. Baes, Jr., "Equilibrium pressure over BeF2/LiF (Flibe) molten mixtures," *Fusion Technology,* 41 (2002) 141.
4. M.R. Zaghloul, D. Sze and A.R. Raffray, "Thermo-physical properties and equilibrium vapor-composition of lithium fluoride-beryllium fluoride (2LiF/BeF_2) molten salt," *Fusion Science and Technology,* **44** (2003) 344-350.
5. R.W. Moir, "Flibe cost estimates," April 29, 1994, internal memo.
6. R.W. Moir, "Flibe cost estimates," September 13,1994, internal memo.
7. D.E. Dombrowski letter, Brush Wellman Inc., August 16, 1994: 35\$/lb at 100 ton/yr sales level.